# PASTEX:

## A Glacio-Meteorological Experiment on the Pasterze (Austria)

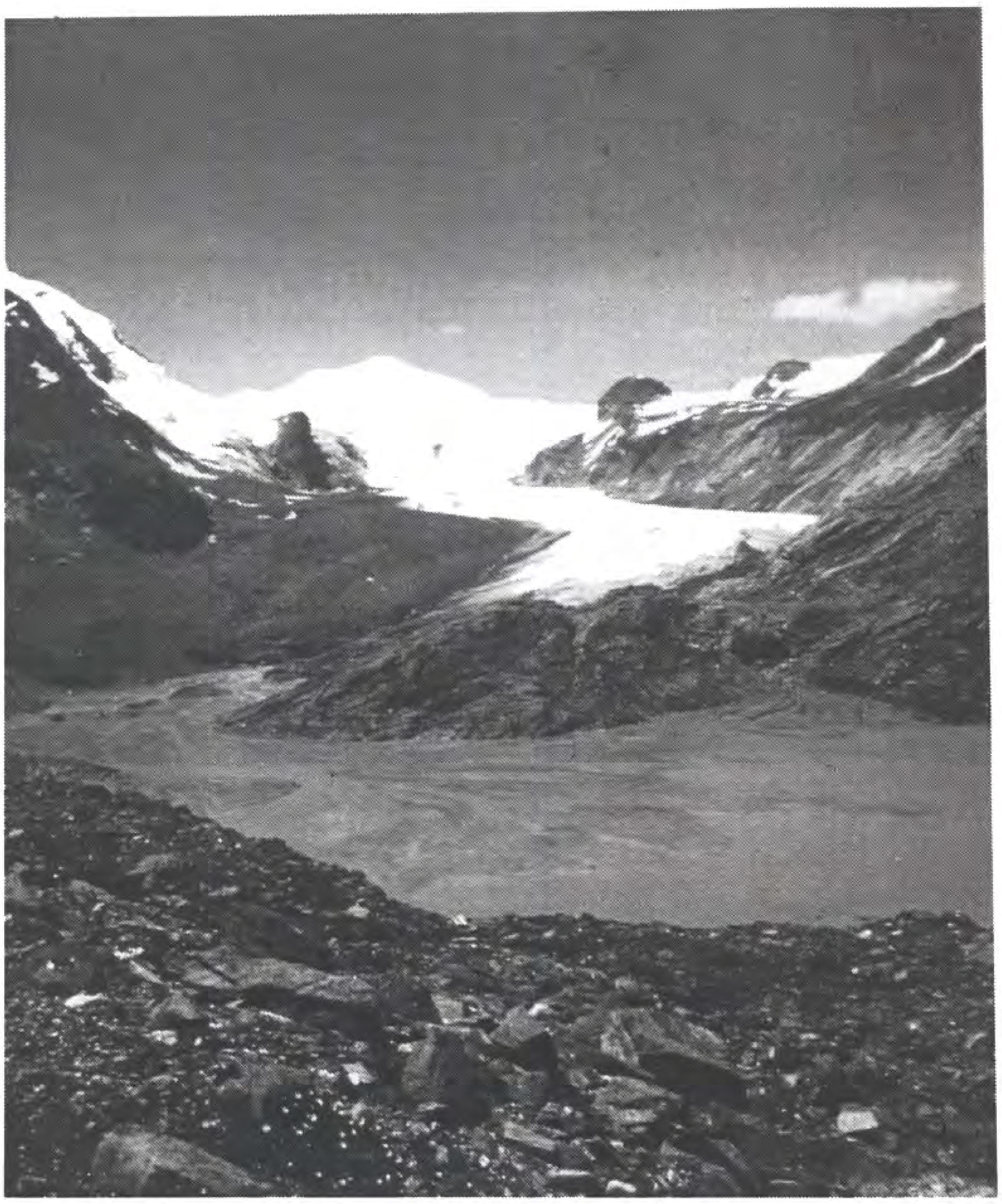

## PASTEX-94 Field Report

Institute for Marine and Atmospheric Research, Utrecht University

Faculty of Earth Sciences, Vrije Universiteit Amsterdam

# PASTEX (PASTerze EXperiment):

# FIELD REPORT ON A GLACIO-METEOROLOGICAL EXPERIMENT ON THE PASTERZE (AUSTRIA)

**Wouter Greuell, Michiel van den Broeke, Wouter Knap, Carleen Reijmer, Paul Smeets and Ingeborg Struijk**

## SUMMARY

A glacio-meteorological experiment (PASTEX) was carried out from mid-June to mid-August 1994 on Austria's largest glacier, Pasterze. Six energy-balance stations were set up along the flow line of the glacier at elevations ranging between 2075 and 3225 m. Mass balance and different components of radiation were measured at all the stations. At most stations profiles of wind speed, temperature and humidity were measured at 0.5 and 2 m. At A1 (2205 m), eddy-correlation measurements were made at two heights and a 13 m mast was erected with profile measurements at eight heights. During PASTEX the mass-balance gradient on the tongue was reversed (i.e. ablation increased with elevation), probably owing to the albedo pattern and an increase in atmospheric temperature with elevation. Measured mass balance can be reproduced by energy-balance calculations within 5 %.

For the study of the circulation in the valley, upper-air soundings were made with a tethered balloon up to a height of 500-1500 m above the launching site at A1. During five days with clear weather and weak geostrophic winds, two maxima were found in the daily variation of the wind speed just above the surface and, during day time, a valley wind developed above the katabatic wind layer.

Inspection of satellite images provides a useful means for the spatial interpolation of point measurements of the albedo. However, methods for retrieval of the surface albedo from space-borne measurements are still under development. Therefore, during PASTEX ground-truth measurements were made in two spectral bands (Landsat 2 and 4), with instruments both with hemispheric and small (5") opening angles.

**CONTENTS**

## PREFACE

The experiment was carried out by staff and students of two institutes. The Faculty of Earth Sciences of the Vrije Universiteit Amsterdam performed the energy-balance measurements at site A1, while the Institute for Marine and Atmospheric Research of the Utrecht University (IMAU) was responsible for the energy-balance measurements at the other sites, the balloon soundings and the spectral albedo measurements.

The field work was performed by the following persons:

| IMAU (Utrecht): | Earth Sciences (Amsterdam): |
|---|---|
| Kees Beets | Hans Bakker |
| Wim Boot | Niek-Jan Bink |
| Michiel van den Broeke | Fred Cannemeijer |
| Louk Conrads | René van Elswijk |
| Henk Dijkstra | Cees Groen |
| Peter Duynkerke | Ron Lootens |
| Wouter Greuell | Paul Smeets |
| Bastiaan Henzing | Ingmar Vollbehr |
| Wouter Knap | Hans Vugts |
| Henk Langedijk | Janette Worm |
| Pieter Luijendijk | |
| Hans Oerlemans | |
| Marcel Portanger | |
| Carleen Reijmer | |
| Ingeborg Struijk | |
| Roderik van de Wal | |
| Jan de Wolde | |
| Zhizheng Zuo | |

### Diary

| | |
|---|---|
| June 1-5 | instruments compared at Cabauw, The Netherlands |
| June 15 | material flown onto the glacier |
| June 15-23 | set up of the energy-balance stations and start of the measurements at U1, U2, U3, U4 and U5 |
| June 18 | start of the energy-balance measurements at A1 |
| June 18-29 | start up of the spectral albedo measurements |
| June 23 | first balloon sounding |
| August 9 | last balloon sounding |
| August 10 | storm blows down mast and damages balloon tent at A1<br>end of the energy-balance measurements at A1 |
| August 12-16 | end of the measurements and take down of the energy-balance stations at U1, U2, U3, U4 and U5 |
| August 16 | material flown off the glacier; permanent weather station and instruments for measuring spectral albedo remain on the glacier |

| | |
|---|---|
| Aug.23 - Sep.5 | instruments compared at Cabauw, The Netherlands |
| October 1 | permanent weather station removed |
| October 1-2 | end of the spectral albedo measurements |


## Acknowledgements

First of all, we would like to thank all the participants in the field work for their enthusiastic and co-operative attitude. The following persons invested many hours in preparation of the expedition: Henk Snellen, co-operators of the Instrumental Group Physics of Utrecht University and co-operators of the Instrumental Group of Theo Hamer and the Electronics Group of Johan de Lange, both of the Faculty of Earth Sciences in Amsterdam. We are very grateful to them. Permissions for the field work were obtained from the ÖAV (Österreichischer Alpenverein), the landowner of the Pasterze, and the "Nationalparkverwaltung", the institution in charge of the management of the national park in which the Pasterze is located. Thank you very much. We also appreciate the help of Gerard van der Vliet, André van Londen and Foeke Kuik, all working for the KNMI (Royal Netherlands Meteorological Institute). The first helped us with organising the field comparison of the instruments at Cabauw and always promptly made the measurements performed by the KNMI at Cabauw available to us. The latter two were of great help during the calibration of our instruments at the KNMI. We thank Leo van Wely from Kipp & Zonen Delft BV for delivering the radiometers in time for the expedition.

The project was financed by the Commission of the European Communities (contract no. EV5V-CT91-0051), the Dutch National Research Programme on Global Air Pollution and Climate Change (contract 276/91-NOP) and the Netherlands Organisation for Scientific Research (NWO/GOA, contract no.750.294.04B).


## Addresses and responsibilities


Wouter Greuell (general field leader and energy-balance measurements), Michiel van den Broeke (balloon soundings), Wouter Knap (measurements of spectral albedo), Hans Oerlemans (general project leader)

Institute for Marine and Atmospheric Research, Utrecht University

Princetonplein 5, NL 3584 CC Utrecht, The Netherlands

Paul Smeets (energy-balance measurements at A1), Hans Vugts (general project leader)

Faculty of Earth Sciences, Vrije Universiteit Amsterdam

De Boelelaan 1085, NL 1081 HV Amsterdam, The Netherlands

## 1. INTRODUCTION

During the last 100 years global mean sea-level rise has been approximately 15 cm (Warrick and Oerlemans, 1990). It is thought that the increase in atmospheric temperature of around 0.5 °C during the same period has caused thermal expansion of the ocean water and a decrease of the land-ice volume. These two processes are believed to have been the main contributors to the observed sea-level rise. The historical volume loss of glaciers has been documented by length measurements, see Figure 1. Obviously, glacier retreat is a world-wide phenomenon.

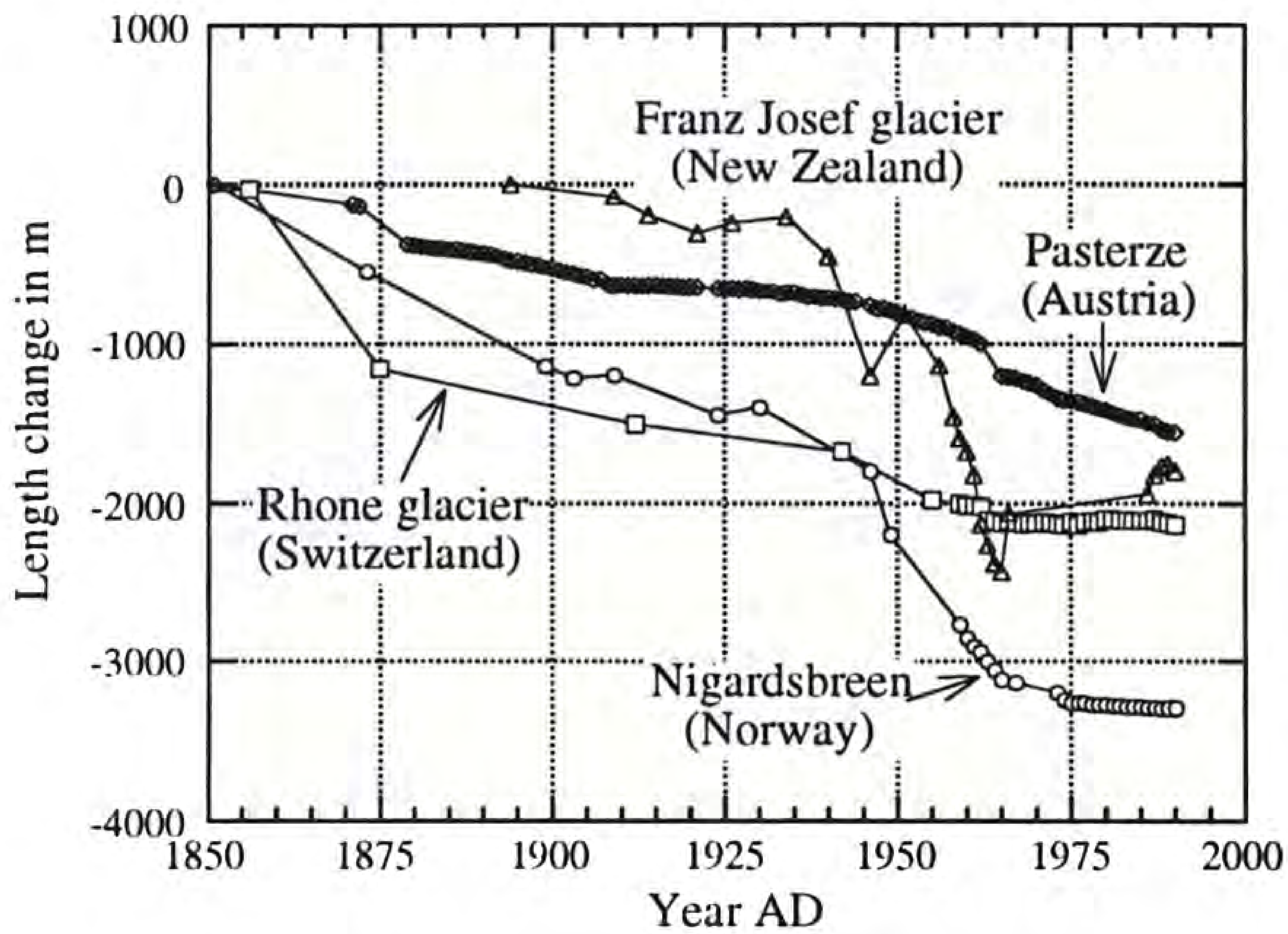


Figure 1: Historical length variations of four glaciers

Owing to the expected continuing increase in the concentration of greenhouse gases, a further and faster rise in temperature is predicted for the near future, say the next 100 years. This will probably lead to an acceleration of sea-level rise and cause problems in low-lying countries like Bangladesh and the Netherlands, unless counter measures like raising of dikes are taken in time.

Predictions of future volume loss of land ice suffer from large uncertainties. It is a task of the scientific community to narrow these uncertainties. With the aim of increasing our knowledge of processes relevant to the climate-glacier-relation, the Faculty of Earth Sciences and the Institute for Marine and Atmospheric Research originally planned a glacio-meteorological experiment on Nigardsbreen, a glacier in Norway, for the summer of 1994. However, during a reconnaissance in 1993 it appeared that access to the tongue of Nigardsbreen was very difficult. It was then decided that this glacier was not suitable for the intended investigations and that the experiment would be performed on the Pasterze.

The Pasterze (47" 06' N and 12" 43' E) is Austria's largest glacier with a surface area of 19.8 km$^2$ and a length of 9.4 km (in 1969 according to Bachmann, 1978). Its general exposure is south-east. A map of the glacier is shown in Figure 2.

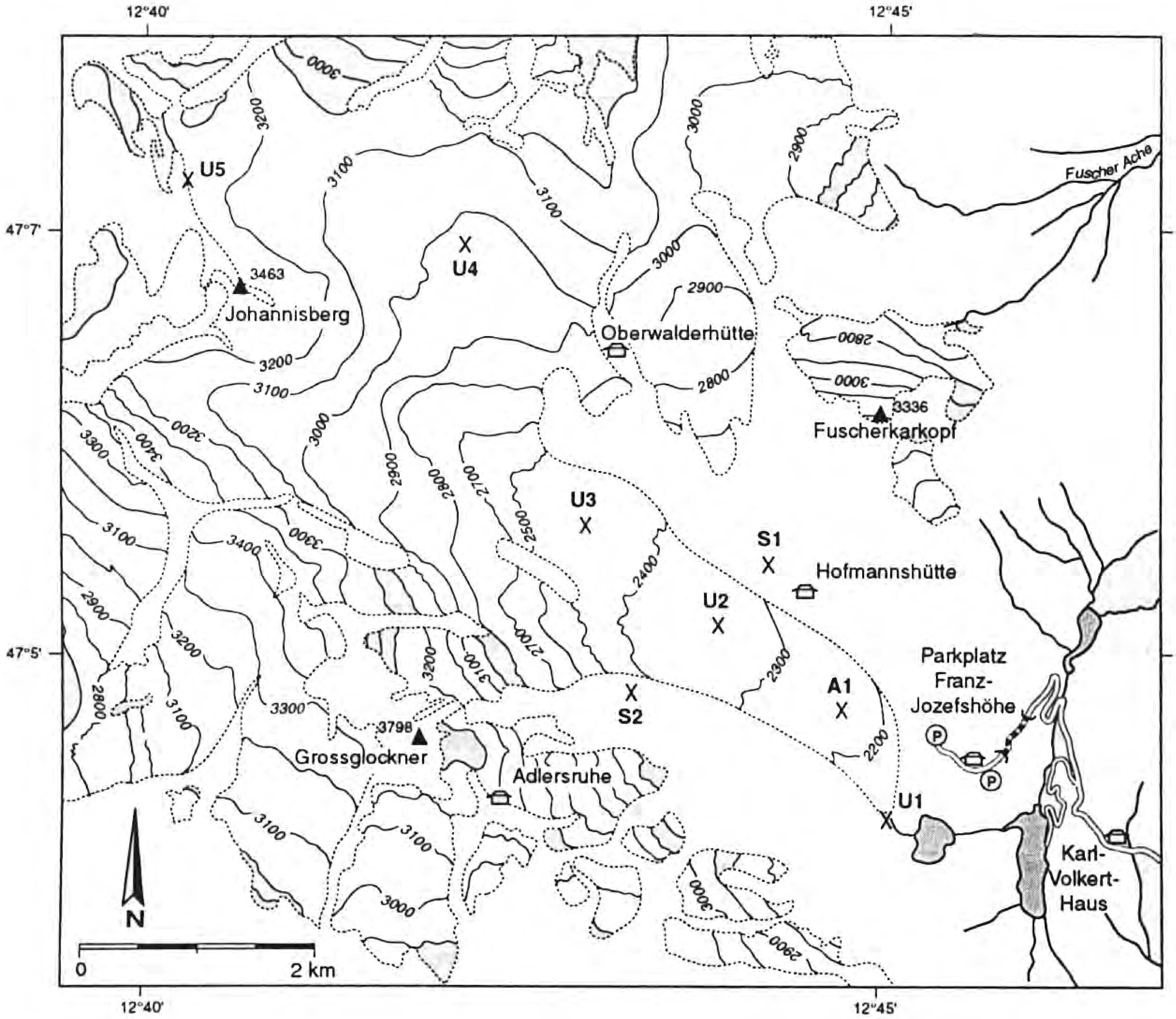


Figure 2: map of the Pasterze

There were several reasons for the choice of the Pasterze for this experiment. The first is its size. A circulation pattern typical for glaciers is more likely to develop above a large than above a small glacier. Secondly, the altitudinal extent of the Pasterze offers the opportunity to study the variation of the mass and energy balance over a relatively large elevation range. PASTEX stations were located between 2075 and 3225 m. An important advantage above many other glaciers is the easy access due to a road ending at a parking lot some 200 m above the tongue and a funicular between the parking lot and the tongue. Both tongue and accumulation basin are relatively flat so that during the experiment it was generally easy to walk to the mast locations.

The last reason for the choice of the Pasterze was the scientific work that had already been done. While knowledge about length variations before 1880 is scarce (Bachmann, 1978), annual length measurements have been performed since that time. Starting in 1926, an increasing number of surface-elevation cross-valley profiles (one in 1926; five at present) is annually being determined at fixed locations (Wakonigg, 1991). Moreover, after some sparse measurements in the years before, mass-balance measurements covering the entire glacier started in 1979 (Tintor, 1991). A run-off station has been operated in the outlet stream of the glacier since 1939. All these measurements are still being continued.

In addition to these measurements, the meteorological station Hoher Sonnblick, at an elevation of 3106 m a.s.l. and approximately 20 km east of the Pasterze, should be mentioned. It has been operated since 1891 and may possibly be used for a reconstruction of the mass-balance history. This has already been done by means of a degree-day approach (Waba, 1993).

The literature contains some other relevant papers and books among which are general descriptions of the glacier and its history (Lang und Lieb, 1993, and Bachmann, 1978), a study of the climate - mass balance - relation (Wakonigg, 1971) and a calculation of some aspects of the velocity pattern of the glacier tongue (Tintor and Wakonigg, 1989).

This field report contains a description of the experimental set up as well as some preliminary results. The experimental set up can be divided into three parts. In order to study the relation between climate and mass balance in a direct way, six energy-balance stations were established along the flow line of the glacier. These stations and the corresponding measurements will be described in Chapter 2.

For obtaining more information about the circulation in the valley and about the relation between variables in the upper air and just above the surface, upper-air soundings were performed with a tethered balloon. These will be described in Chapter 3.

In order to verify and improve techniques for the retrieval of albedo by Landsat images, three stations were established on and near the glacier. A description will be given in Chapter 4.

The measurements performed on the Pasterze are a continuation of previous energy-balance measurements on glaciers and ice sheets done by the institutes participating in the experiment. An overview is given in Table 1.

Table 1: previous energy-balance measurements on glaciers and ice sheets done by the institutes participating in the experiment.

| ablation season of | location | references |
|---|---|---|
| 1986 | Hintereisferner, Austria | Greuell and Oerlemans, 1989 |
| 1989 | Hintereisferner, Austria | Van de Wal, Oerlemans and Van der Hage, 1992 |
| 1990/1991 | Ecology Glacier, King George Island, Antarctica | Bintanja et al., 1991<br>Bintanja, 1995 |
| 1990 and 1991 | West Greenland | Bintanja et al., 1990<br>Boot et al., 1991<br>Oerlemans and Vugts, 1993 |
| 1992/1993 | Heimefront Range, Antarctica | Bintanja et al., 1993<br>Bintanja and Van den Broeke, 1995 |

## 2. ENERGY-BALANCE MEASUREMENTS

### 2.1. Introduction

The idea behind energy-balance measurements on glaciers is to link climate to glacier melt. On glaciers this is done by determining the energy fluxes between the atmosphere and the surface and the energy fluxes and sinks in the ice or snow. The energy exchange between the atmosphere and the surface is due to radiative fluxes, which can be measured directly, and to turbulent fluxes. The latter can be determined directly by eddy-correlation measurements, or indirectly by combining measurements of wind speed, temperature and humidity profiles with calculations with a theory relating these profiles to the fluxes. Under the conditions met during PASTEX, the energy coming in from the atmosphere was used to melt snow or ice in the uppermost layers of the glacier. Therefore, the amount of melt can be calculated from the incoming energy fluxes and then be compared with the measured amount of melt. In reality, the energy balance is a bit more complicated owing to sub-surface conductive and radiative fluxes.

When ambient temperatures are higher than the melting point of ice, the air mass just above the glacier surface cools down. Since the density of air increases with decreasing temperature, this air mass starts to flow down along the glacier. The resulting katabatic wind (or glacier wind) is a typical phenomenon during summer for glaciers in the Alps. Within the katabatic wind layer, vertical profiles of wind speed, temperature and humidity, and therefore of the turbulent fluxes, differ markedly from "normal profiles". The set up of the energy-balance station at A1 was meant to study this feature in detail.

## 2.2. Set up

Six energy-balance stations were established along the flow line of the glacier (see Figure 2), two in the upper part of the glacier (U4 and U5), three on the tongue (A1, U2 and U3) and one on the end moraine just some 10 m away from the front (U1). Table 2 lists the elevations of the stations, the variables measured and the sensors used. The profile of the glacier along the flow line is shown in Figure 3.

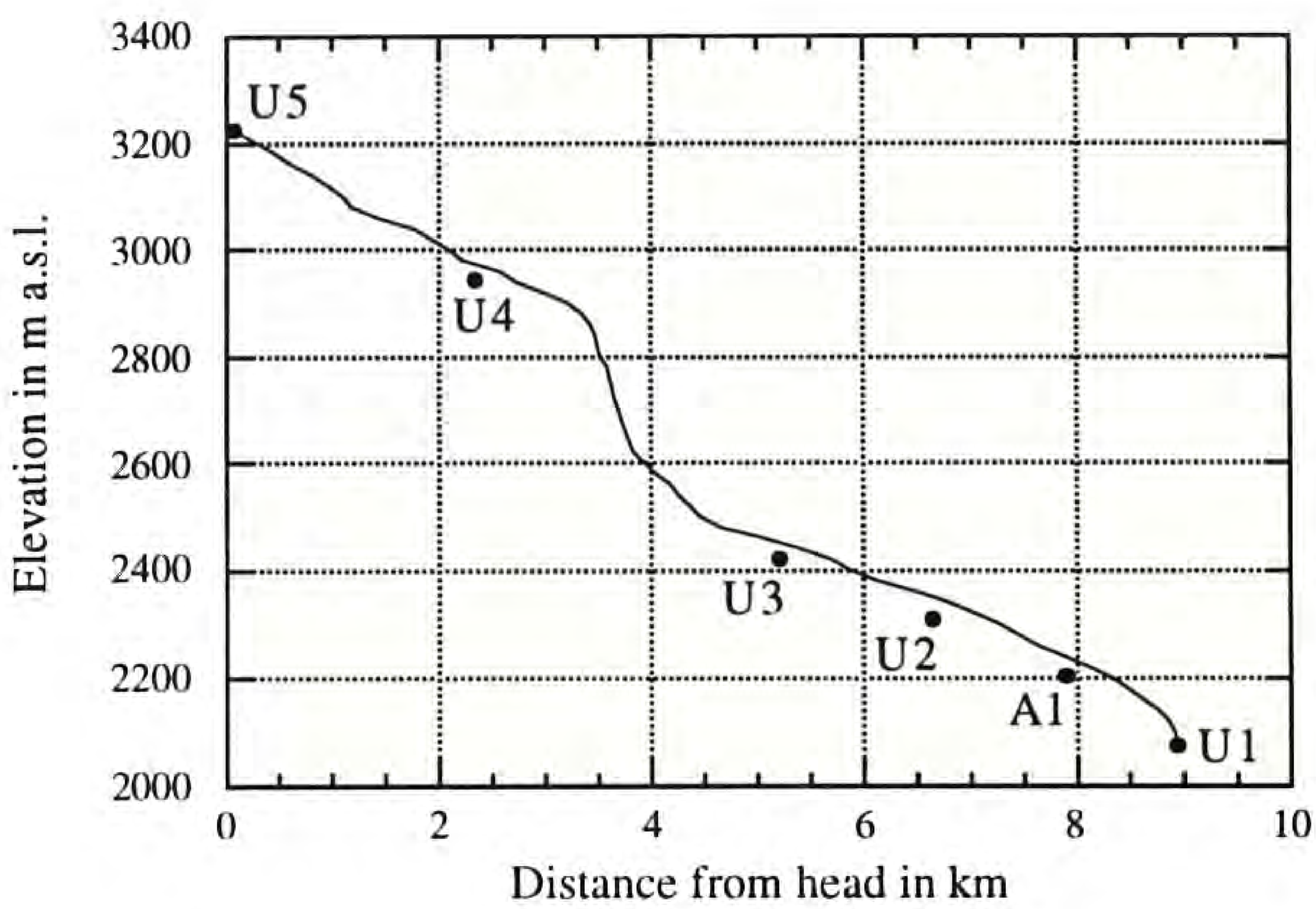


Figure 3: Profile of the Pasterze along the flow line with mast locations. Some mast locations seem to be below the surface since surface elevations are those for 1985 while the elevations of the mast locations were determined in 1994.

The main station was located at A1, where radiative fluxes were measured for all short- and long-wave components and as net radiation. Profile measurements of wind speed, temperature and humidity were made at eight levels along a 13 m mast and turbulent fluxes were measured directly by eddy correlation at 10 and 4 (or 2.5) m on two separate

Table 2: elevation of the stations, variables measured, heights of the measurements and instrument types used.

| | |
|---|---|
| Aand. | Aanderaa: wind speed sensor 2740; wind direction sensor 3150; temperature sensor 3145; total radiation sensor 2811 |
| Camp. | Campbell Q7 net radiometer |
| Eppley | Eppley pyrgeometer, model PIR |
| Gill | Gill Instruments, ultrasonic anemometer |
| HMP | HMP35AC temperature and relative humidity probe |
| Kipp | Kipp pyranometer: CM7 at A1 and CM 14 at the "U-stations" |
| Lyman | Lyman $\alpha$ hygrometer (Free University Amsterdam) |
| Rotr. | Rotronix, model MP-100F |
| Schulze | Schulze net radiometer |
| thc. | thermocouples (Agricultural University Wageningen and Free University Amsterdam) |
| VI | Vector Instruments: A 100 R cup anemometer and W 200 P wind vane |

all sensors marked with an asterisk were ventilated
&: but 92.5 % misses at 13 m $: but 0.5 % misses at 2.5 m

| Station | elevation in m a.s.l. | data logger system | period | variables measured | missing data in % |
|---|---|---|---|---|---|
| U1 | 2075 | RIDAS | Jun.17-Aug.12 | total radiation: incoming and outgoing (Aand.)* | 0.1 |
| | | | | temperature: 0.5 and 2 m (Aand.)* | 0.1 |
| | | | | humidity: 2 m (Rotr.)* | 0.5 |
| | | | | wind speed: 0.5 and 2 m (Aand.) | 0.1 |
| | | | | wind direction: 2 m (Aand.) | 0.1 |
| | | RIDAS | Jun.20-Aug.11 | subsurface temperature: 2, 2, 5, 12.5 and 30 cm (Pt500) | 0.2 |
| | | MIDAS | Jun.17-Aug.12 | short wave radiation: incoming and outgoing (Kipp) | 0.0 |
| | | | | temperature: 0.5 and 2 m (HMP)* | 0.0 |
| | | | | humidity: 0.5 and 2 m (HMP)* | 0.0 |
| A1 | 2205 | | Jun.18-Aug.9 | short wave radiation: incoming and outgoing (Kipp) | 0.0 |
| | | | Jun.18-Aug.9 | long wave radiation: incoming and outgoing (Eppley) | 0.0 |
| | | | Jun.18-Aug.9 | total radiation: net (Schulze and Camp.) | 0.0 |
| | | | Jun.18-Aug.11 | wind fluctuations, 4 (or 2.5) and 10 m (Gill) | 27.5 |
| | | | Jun.18-Aug.11 | temperature fluctuations, 4 (or 2.5) and 10 m (Gill and thc.) | 27.5 |
| | | | Jun.18-Aug.11 | humidity fluctuations, 4 (or 2.5) and 10 m (Lyman) | ±90.0 |
| | | | Jun.16-Aug.9 | temperature, 0.25, 0.5, 1, 2, 4, 6, 8 and 13 m (HMP)* | 0.0 |
| | | | Jun.16-Aug.9 | humidity, 0.25, 0.5, 1, 2, 4, 6, 8 and 13 m (HMP)* | 0.0& |
| | | | Jun.18-Aug.9 | wind speed, 0.25, 0.5, 1, 2, 4, 6, 8 and 13 m (VI) | 0.0 |
| | | | Jun.18-Aug.9 | wind direction, 2.5 and 13 m (VI) | 0.0$ |

| | | | | | |
|---|---|---|---|---|---|
| U2 | 2310 | RIDAS | Jun.17-Aug.12 | total radiation: incoming and outgoing (Aand.)* | 5.8 |
| | | | | temperature: 0.5 and 2 m (Aand.)* | 5.8 |
| | | | | humidity: 2 m (Rotr.)* | 8.1 |
| | | | | wind speed: 0.5 and 2 m (Aand.) | 5.8 |
| | | | | wind direction: 2 m (Aand.) | 5.8 |
| | | MIDAS | Jun.19-Aug.12 | short wave radiation: incoming and outgoing (Kipp) | 1.8 |
| | | | | long wave radiation: incoming (Eppley)* | 1.8 |
| | | | | temperature: 0.5 and 2 m (HMP)* | 1.8 |
| | | | | humidity: 0.5 and 2 m (HMP)* | 1.8 |
| U3 | 2420 | RIDAS | Jun.19-Aug.12 | temperature: 0.5 and 2 m (Aand.)* | 0.1 |
| | | | | humidity: 2 m (Rotr.)* | 1.0 |
| | | | | wind speed: 0.5 and 2 m (Aand.) | 0.1 |
| | | | | wind direction: 2 m (Aand.) | 0.1 |
| | | MIDAS | Jun.23-Aug.12 | short wave radiation: incoming and outgoing (Kipp) | 0.0 |
| U4 | 2945 | RIDAS | Jun.15-Aug.14 | temperature: 0.5 and 2 m (Aand.)* | 1.0 |
| | | | | humidity: 2 m (Rotr.)* | 23.2 |
| | | | | wind speed: 0.5 and 2 m (Aand.) | 2.6 |
| | | | | wind direction: 2 m (Aand.) | 17.2 |
| | | MIDAS | Jun.16-Aug.16 | short wave radiation: incoming and outgoing (Kipp) | 0.0 |
| U5 | 3225 | RIDAS | Jun.15-Aug.14 | temperature: 0.5 and 2 m (Aand.)* | 1.6 |
| | | | | humidity: 2 m (Rotr.)* | 53.2 |
| | | | | wind speed: 0.5 and 2 m (Aand.) | 12.3 |
| | | | | wind direction: 2 m (Aand.) | 4.7 |
| | | MIDAS | Jun.15-Aug.16 | short wave radiation: incoming and outgoing (Kipp) | 0.0 |
| | | | | long wave radiation: incoming (Eppley)* | 0.0 |
| | | | | temperature: 0.5 and 2 m (HMP)* | 0.0 |
| | | | | humidity: 0.5 and 2 m (HMP)* | 0.0 |

masts. Measurements of wind direction took place at 13 and 2 m. At this location the balloon soundings (see Chapter 3) were also made.

At the other locations (U1, U2, U3, U4 and U5; the "U-stations") a smaller amount of variables was measured. With respect to the radiative fluxes, the short-wave components were registered at all the "U-stations", incoming long wave radiation was measured at U2 and U5 and the incoming and the outgoing total radiation at U1 and U2. Wind speed, temperature and humidity were measured at 0.5 and 2 m (but at U3 and U4 humidity was not measured at 0.5 m).

The meteorological mast at U5 (3225 m)

Table 2 also shows the distribution of the sensors over the different data-logger systems. With RIDAS (Radio Interfacing Data Acquisition System) samples were taken every 2 minutes (the integral over 2 minutes for wind speed). The data were collected by a self-made data logger and under "normal conditions" approximately every 45 minutes they were transmitted to the computer in the hotel (Karl-Volkert-Haus). Owing to specific weather conditions, the signal was not always received in the hotel. In those cases, new attempts to transmit were made later on by the system. This was possible because during a maximum of 24 hours unreceived data were stored in the data loggers at the masts. As a result, hardly any data got lost owing to transmittance problems.

The data collected by the MIDAS (Memory Interfacing Data Acquisition System) system are all 2-minutes averages of samples taken every 10 seconds. These data were stored on memory cards by Campbell data loggers. About every week, the cards were exchanged and the data read into a computer, although the capacity of the cards was enough for approximately 6 weeks of data.

With the exception of the eddy-correlation measurements, at A1 samples were taken every 30 seconds by three data loggers (Campbell, 21x Micro logger). These samples were averaged over 5 minutes. Each half hour, these 5 minutes samples were averaged and the results were dumped on an external storage device.

Two sampling procedures were used for the eddy-correlation measurements. Firstly, a data logger was sampling every second during the whole period. Secondly, during parts of the period sampling took place at a rate of 10 Hz with the aid of a microcomputer system. These data were dumped on tapes.

At A1, the masts for the eddy-correlation, radiation and profile measurements were drilled into the ice and levelled almost every day. The masts at the other locations were standing on four legs ending in pins perpendicular to the legs. These masts were put on the surface and the instruments were set horizontal. The legs melted down some 10 to 20 cm into the snow or ice and thereafter the position of the mast relative to the surface remained the same within a few centimetres, unless heavy snow-fall events occurred. This system has two advantages: no drilling is needed and without human interference the height of the instruments above the surface hardly varies. Tilt caused by differential melting at the four legs constitutes a potential drawback of this construction. However, during PASTEX the amount of tilt was small. A maximum of 1° for the short-wave radiation sensors occurred, as shown by tilt measurements performed each time the masts were visited.

In order to complete the energy balance, the so-called mass balance, which is roughly the amount of snow fall minus the amount of melt, was determined at each location on the glacier. For this purpose, five stakes with a mutual distance of approximately 10 m were established within 50 m of each glacier mast. Snow-density profiles were regularly measured as long as the surface was snow covered (at U4 and U5 during the whole period and at U3 during the first 7-10 days of the measurements). Instead of the mass balance, sub-surface temperatures were measured on the moraine at U1, since at this location the energy exchange with the atmosphere results in heating or cooling below the surface.

Two other kinds of data collected during the experiment should be mentioned. Precipitation was automatically recorded with a Campbell rain gauge at A1 (June 18-August 11). Cloud observations (total cloud amount, cloud amount due to low clouds, cloud amount due to middle clouds, cloud amount due to high clouds, cloud type and cloud-base elevation) were made every three hours, except during the night.

Table 3: Measurements made with the PWS at U2 from August 16 to October 1, 1994.

| Variables measured | sensors types | sample frequency (once per ...) |
|---|---|---|
| incoming short-wave radiation | Aanderaa 2770 | 10 minutes |
| outgoing short-wave radiation | Aanderaa 2770 | 10 minutes |
| temperature | Aanderaa 3145 | 10 minutes |
| wind speed | Aanderaa 2740 | 1 hour (integral) |
| wind direction | Aanderaa 3150 | 1 hour |
| air pressure | Aanderaa 2810 | 1 hour |

Mid-August all the masts were removed. However, at U2 a so-called "Permanent Weather Station" (PWS) was left behind, that was operated from August 16 until October 1, 1994. The variables measured, the instruments employed and the frequencies of the measurements are listed in Table 3. All the measurements were taken at a height of approximately 4 m above the surface. The temperature sensor was unventilated. Hourly means of the samples were both locally stored on a Campbell storage module (SM 716) and transmitted to Utrecht by ARGOS. Fortunately, the local storage system was successful because many data would have been lost if only the ARGOS system had been used. The sensors were mounted on a four-legged mast of the type described before. The PWS resembles the PWS's currently operated by the IMAU on the Greenland Ice Sheet.

## 2.3. Calibration and comparison of the instruments and accuracy of the measurements

Before the expedition, in April 1994 , the following sensors used at the "U-stations" were calibrated at the KNMI (Royal Netherlands Meteorological Institute): wind speed, temperature (both HMP's and Aanderaa's), humidity (both HMP's and Rotronix) and short-wave radiation. The wind speed sensors used at A1 were calibrated just before and after (May and August, 1994) the expedition in a wind-tunnel system at the Department of Meteorology of the Agricultural University Wageningen.

Just before (June 1 - June 5) and after (August 23 - September 5) the expedition, all the instruments used on the Pasterze were set up for comparative measurements. This was done near the 200 m micro-meteorological tower in Cabauw, located approximately 20 km south-west of Utrecht and run by the KNMI. Instruments measuring the same variables were put at the same height. In most cases, this height coincided with that of one of the KNMI sensors. Owing to shadow effects of other instruments and the masts themselves, comparison of the wind sensors was not meaningful.

Accuracy's provided by the manufacturers are listed in Table 4.

Table 4: accuracy's of the instruments according to the manufacturers.

| Instrument | accuracy |
|---|---|
| Aanderaa air-pressure sensor 2810 | 0.2 hPa |
| Aanderaa pyranometer 2770 | better than 20 $Wm^{-2}$ |
| Aanderaa wind-direction sensor 3150 | better than 5° |
| Aanderaa wind-speed sensor 2740 | maximum of 2 % and 0.2 m/s |
| Campbell ARG100 tipping bucket rain gauge | 0.2 mm/tip |
| Campbell Q7 net radiometer | better than 3 % |
| Gill Instruments, ultrasonic anemometer | 1.5 % ( for a 10 s average) |
| HMP35AC temperature probe | 0.2 °C |
| HMP35AC relative humidity probe | 2 % RH for 0 to 90 % RH;<br>3 % RH for 90 to 100 % RH |
| Kipp CM 7 pyranometer | better than 3 % |
| Lyman alpha hygrometer (self-made) | 10 % (for the fluctuations) |
| Rotronix, humidity probe, model MP-100F | 1.5 % RH |
| Schulze net radiometer | better than 3 % |
| thermocouples (self-made) | 2 % (for the fluctuations) |
| Vector Instruments, A 100 R cup anemometer | 0.1 m/s |
| Vector Instruments, W 200 P wind vane | 2 degrees |

## 2.4. Period of the measurements and missing data

Table 2 gives the periods of the measurements and the percentages of missing data during these periods. The main causes of data losses are:

- rotation of the wind-speed and wind-direction sensors was hindered by ice deposition. This only occurred at U4 and U5;
- the Rotronix humidity sensors reached their maximum output value at relative humidities less than 100 %. This occurred mainly at U2, U4 and U5;
- electronic problems with both kinds of data loggers (RIDAS and MIDAS) at U2;

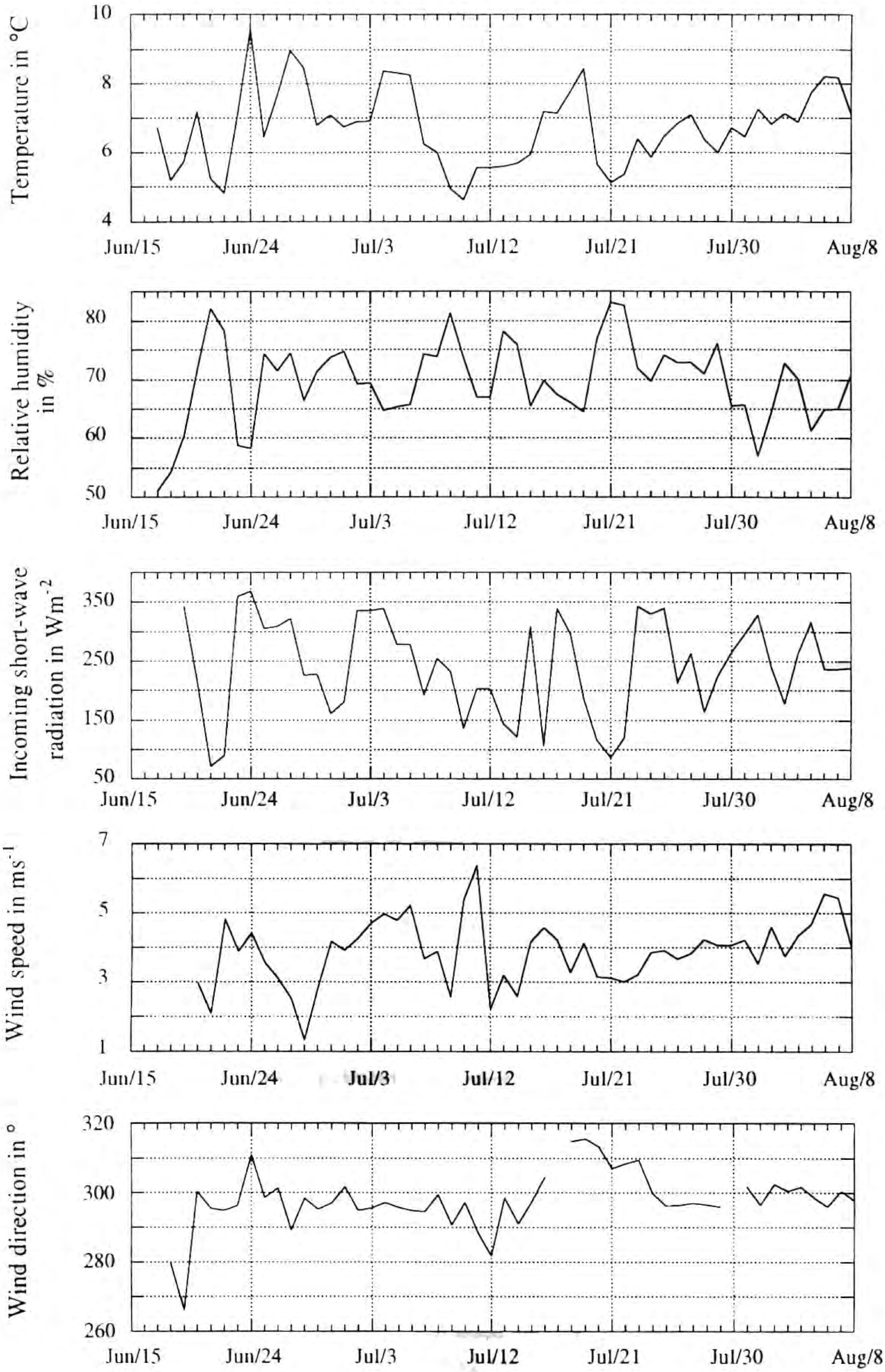


Figure 4: daily mean temperature, incoming short-wave radiation, relative humidity, 2 m-wind velocity and 2 m-wind direction at A1.

- problems with individual sensors, namely the wind-direction sensor at U4 and the Rotronix humidity sensor at U5;
- problems with the generator at A1;
- sonic anemometer data obtained during rain fall could not be used;
- sonic anemometer data collected while the masts were levelled could not be used;
- the humidity sensors placed at 13 m at A1 were damaged twice by lightning in the beginning of the period;
- the two Lyman alpha hygrometers at A1 didn't operate well owing to leakage of the Lyman alpha light bulbs;
- on several occasions, thermocouples at A1 were damaged by rain and hail.

## 2.5. Some preliminary results

### 2.5.1. Daily means

Figure 4 shows the daily mean temperature, incoming short-wave radiation, relative humidity, wind velocity and wind direction for A1.

### 2.5.2. The wind field

Apparently, the glacier wind dominates at A1. To get a better impression of the distribution of the wind over the different directions, histograms of the half-hourly mean wind direction were constructed. These histograms are shown in Figure 5. Obviously, the glacier-wind direction dominates at all masts. Only at U5, located near the glacier head, other directions are frequent too. Peaks in the distribution are found around 110° and 290°. This is mainly due to the local topography. The two directions are opposite to each other and almost perpendicular to the mountain ridge. The influence of the large-scale circulation on the measured wind field at U5 was studied by comparing the 500 hPa geostrophic wind (calculated with data of the ECMWF) at 12:00 GMT (14:00 Local Time) with the daily mean wind velocity and direction at U5 (see Figure 6). The scatter plot of the wind velocity shows that a geostrophic wind weaker than 10 $ms^{-1}$ hardly influences the measured wind velocity. Above this wind velocity there is a relationship; these points are marked in the scatter plot of the wind direction. The measured wind direction in almost all of these points is approximately 290°, while the geostrophic wind direction is around 260°. A geostrophic wind of around 150° mostly results in a measured wind of 100°. These rotations are probably due to the local topography.

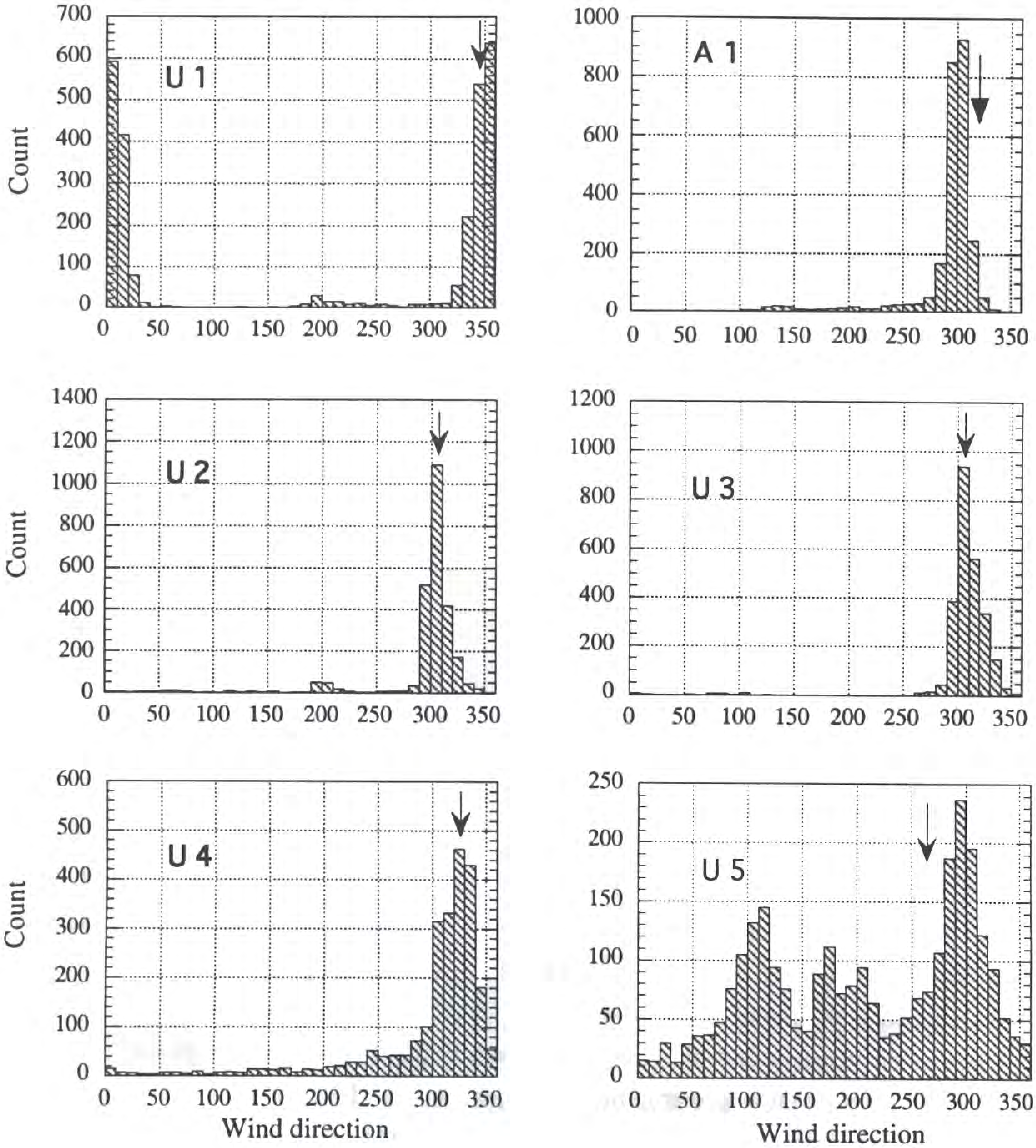


Figure 5: half-hourly mean wind directions at the six masts. Down-valley directions are indicated by arrows.

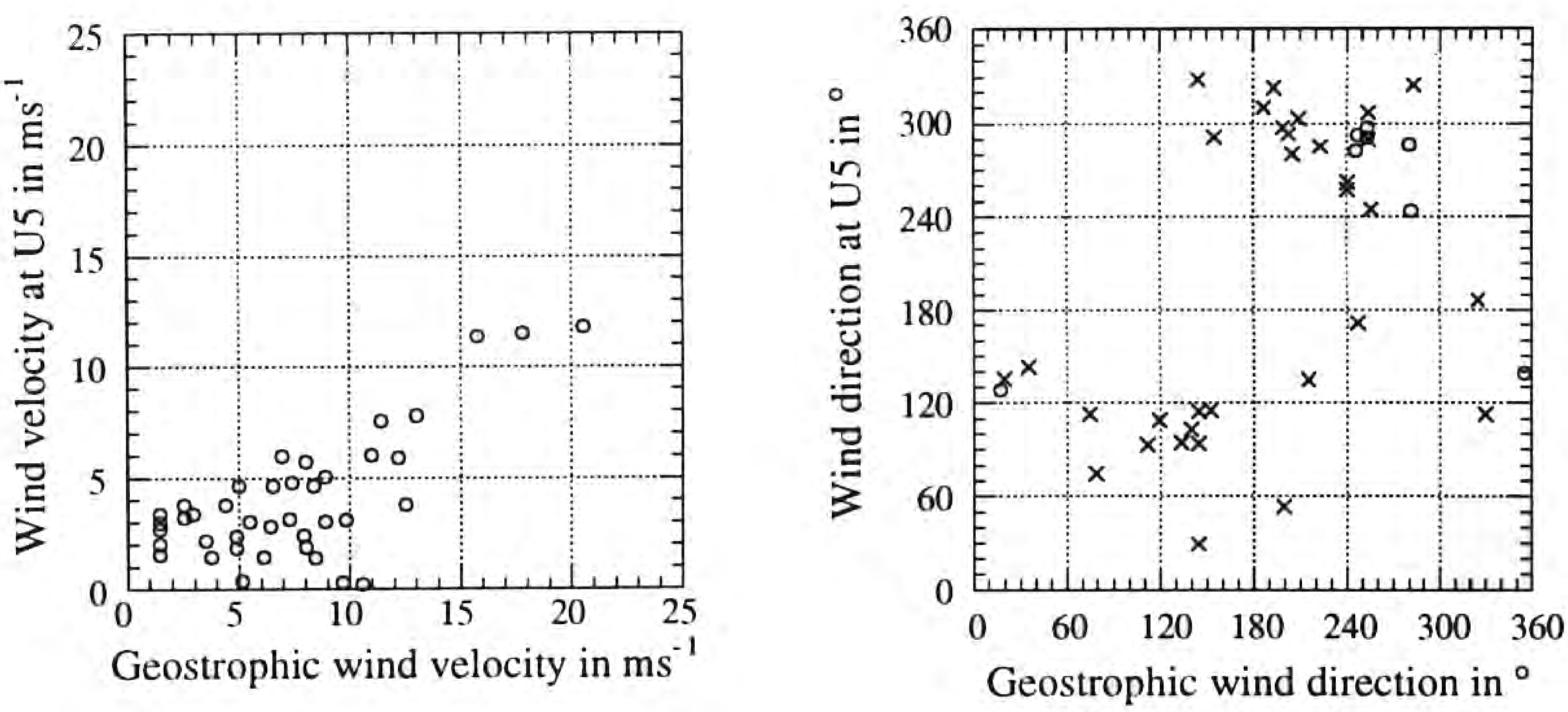


Figure 6: comparison of the geostrophic wind at 500 hPa at 14:00 Local Time with the daily mean wind at U5. In the wind-direction panel, crosses correspond to geostrophic wind speeds less than 10 $ms^{-1}$ and circles correspond to larger geostrophic wind speeds.

### 2.5.3. Variations with elevation

The variations of some measured elements with elevation are depicted in Figure 7. For the mass-balance rate this is the average between June 21 and August 8 while for the meteorological elements all those samples, which coincide with simultaneous measurements of the same elements at all the other stations, are averaged. Therefore, different curves in the figure cover almost, but not exactly, the same period. Here, the discussion of the figure focuses on variations on the tongue.

During PASTEX the ablation rate on the tongue (where no accumulation occurred) increased with elevation. However, a decade of measurements of the net mass balance on Pasterze (Tintor, 1991) shows the usual increase with elevation. Maybe, the apparent contradiction is due to a large accumulation gradient on the tongue.

The reversed mass-balance gradient can partly be explained by the variation of the meteorological elements with elevation. Three reasons for the higher ablation at U3 as compared to U2 can be distinguished. The first factor is higher global radiation and can to some extent be ascribed to a shorter path through the atmosphere at higher elevations. The second factor is a lower albedo and is unusual. Commonly, the albedo increases with elevation. Possibly, this is an effect of the nearby ice fall. Inspection of LANDSAT images should show whether or not the albedos measured at the masts are representative for the variations on the tongue. The third factor causing higher melt rates at U3 as compared to U2 are higher temperatures.

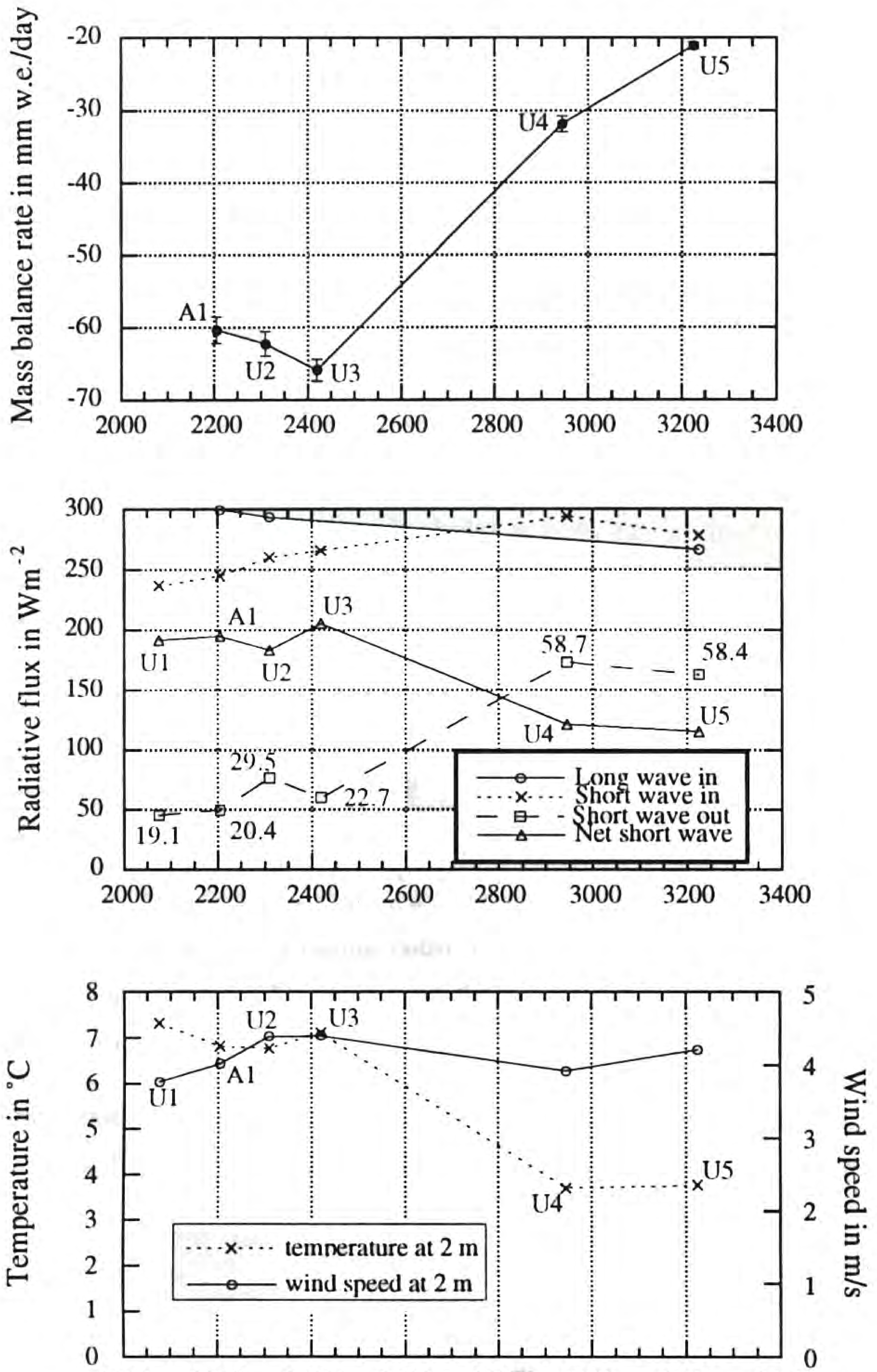


Figure 7: variation with elevation of the mass-balance rate and several meteorological elements during PASTEX. For the mass-balance rate this is the average between June 21 and August 8 while for the meteorological elements all those samples, which coincide with simultaneous measurements of the same elements at all the other stations, are averaged.

At first sight, it is difficult to explain the increase in ablation rate from A1 to U2. Net radiation is smaller at U2 than at A1 while the temperature is almost equal. However, higher wind speeds certainly caused more melt at U2. Moreover, the surface at U2 was rougher, so that probably roughness lengths and therefore turbulent fluxes are larger at this location as compared to A1. In future, roughness lengths for all the stations will be calculated from the available profile data.

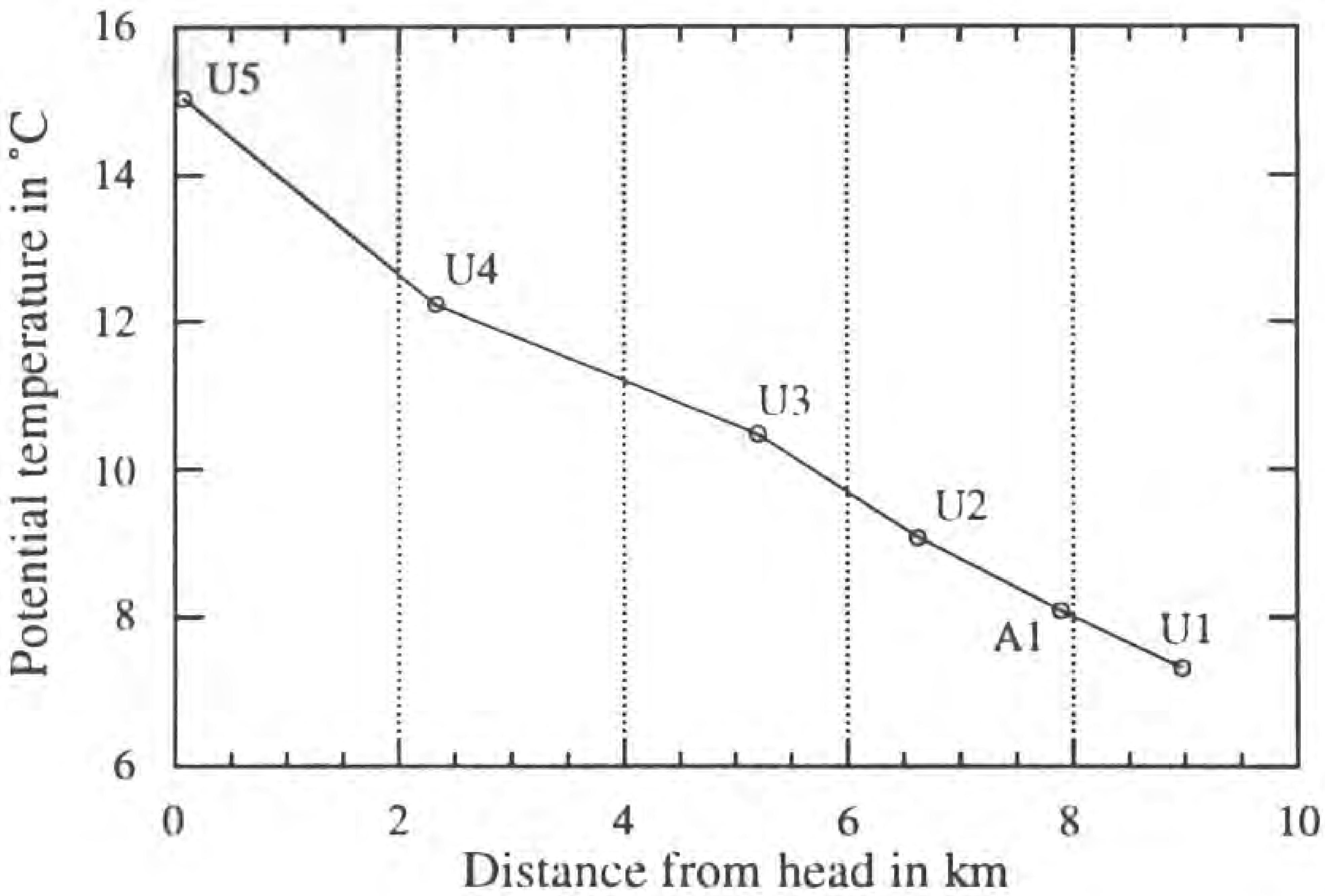


Figure 8: Potential temperature as a function of the distance from the glacier head. All those temperature measurements, which coincide with simultaneous measurements at all the other stations, are averaged.

Much of the change of the 2 m temperature with elevation can be understood when the 2 m potential temperature is plotted against the distance along the glacier (Figure 8). The irregular curve turns into a rather smooth curve, which contains qualitative information about relevant thermodynamic processes. Making the assumptions of a stable stratification, the wind directed along the glacier flow line and unsaturated air, an air mass flowing down (or up) along the glacier surface changes its temperature in three ways: 1. it warms (or cools) adiabatically, 2. it cools owing to exchange of sensible heat with the surface and 3. it warms owing to entrainment. According to Figure 8 the 2 m potential temperature decreases strongly with decreasing elevation. As adiabatic warming and cooling do not affect potential temperature, it can be concluded that at the 2 m level exchange of sensible heat with the surface is much more effective than entrainment.

The meteorological mast at U3 (2420 m)

### 2.5.4. Mass-balance calculations

In this section the measured mass balance at the five glacier locations will be compared to the mass balance calculated with an energy-balance model, namely that described in Greuell and Konzelmann (1994).

Important aspects of the calculations are:

- the model consists of two parts. The first describes the energy fluxes between the atmosphere and the glacier; the second calculates temperature, density and water content in the uppermost 25 m of the glacier on a vertical, 1D, grid. Englacial processes simulated include conduction, radiation penetration, melting, and percolation, refreezing and run-off of melt water. The surface temperature is also calculated and plays an important role in linking the two parts of the model;

- the model was forced by the following, measured, variables: 2 m temperature, 2 m humidity, 2 m wind speed, incoming short-wave radiation, outgoing short-wave radiation and incoming long-wave radiation;
- outgoing long-wave radiation was calculated from the calculated surface temperature;
- the turbulent fluxes were calculated with the Monin-Obukhov similarity theory using the equations given by Businger et al. (1971) and the parameterization scheme for the surface roughness lengths used in Greuell and Konzelmann (1994). Therefore, the momentum roughness length is 3.2 mm for ice and 1.3 mm for snow while the roughness lengths for temperature and water vapour are 0.01 mm;
- uncertainties in the initial profiles of temperature, density and water content probably do not substantially affect the mass-balance calculations.

Table 5: comparison of measured and calculated mass balance (m.b.) during PASTEX. The energy fluxes given (in $Wm^{-2}$) are means for the entire period and are partly measured, partly calculated.

| Location, elevation in m a.s.l. | A1, 2205 | U2, 2310 | U3, 2420 | U4, 2945 | U5, 3225 |
|---|---|---|---|---|---|
| period | 18/6-7/8 | 21/6-12/8 | 19/6-12/8 | 15/6-16/8 | 15/6-16/8 |
| measured m.b. in mm w.e. | -2962 | -3279 | -3512 | -1845 | -1220 |
| calc.-meas. m.b. in mm w.e. | -25 (-1%) | +117 (4%) | +113 (3%) | -89 (5%) | -51 (4%) |
| incoming short-wave radiation | 246.7 | 262.2 | 263.9 | 297.0 | 279.2 |
| outgoing short-wave radiation | 52.4 | 77.1 | 65.3 | 178.1 | 170.1 |
| albedo in % | 21.2 | 29.4 | 24.7 | 60.0 | 60.9 |
| incoming long-wave radiation | 299.4 | 298.8 | 296.8 | 281.3 | 273.6 |
| outgoing long-wave radiation | 314.9 | 315.4 | 315.4 | 313.8 | 312.4 |
| net total radiation | 178.8 | 168.5 | 180.0 | 86.4 | 70.3 |
| sensible heat flux | 45.0 | 56.4 | 53.3 | 19.8 | 18.6 |
| latent heat flux | 8.8 | 11.6 | 8.7 | 3.4 | -1.6 |
| total energy flux | 232.6 | 236.5 | 242.0 | 109.6 | 87.3 |

Results of the computations are given in Table 5. Calculated and measured mass balance do not differ by more than 5 %. Figure 9 gives some details about the simulation for A1. Apparently (lower panel), measured variations in ablation rate between stake readings can be reproduced reasonably well by the calculations (corr.coeff.=0.83). Much of the scatter around the 1:1 line is due to the uncertainty in the measurement given as the standard deviation of the values from the five stakes.

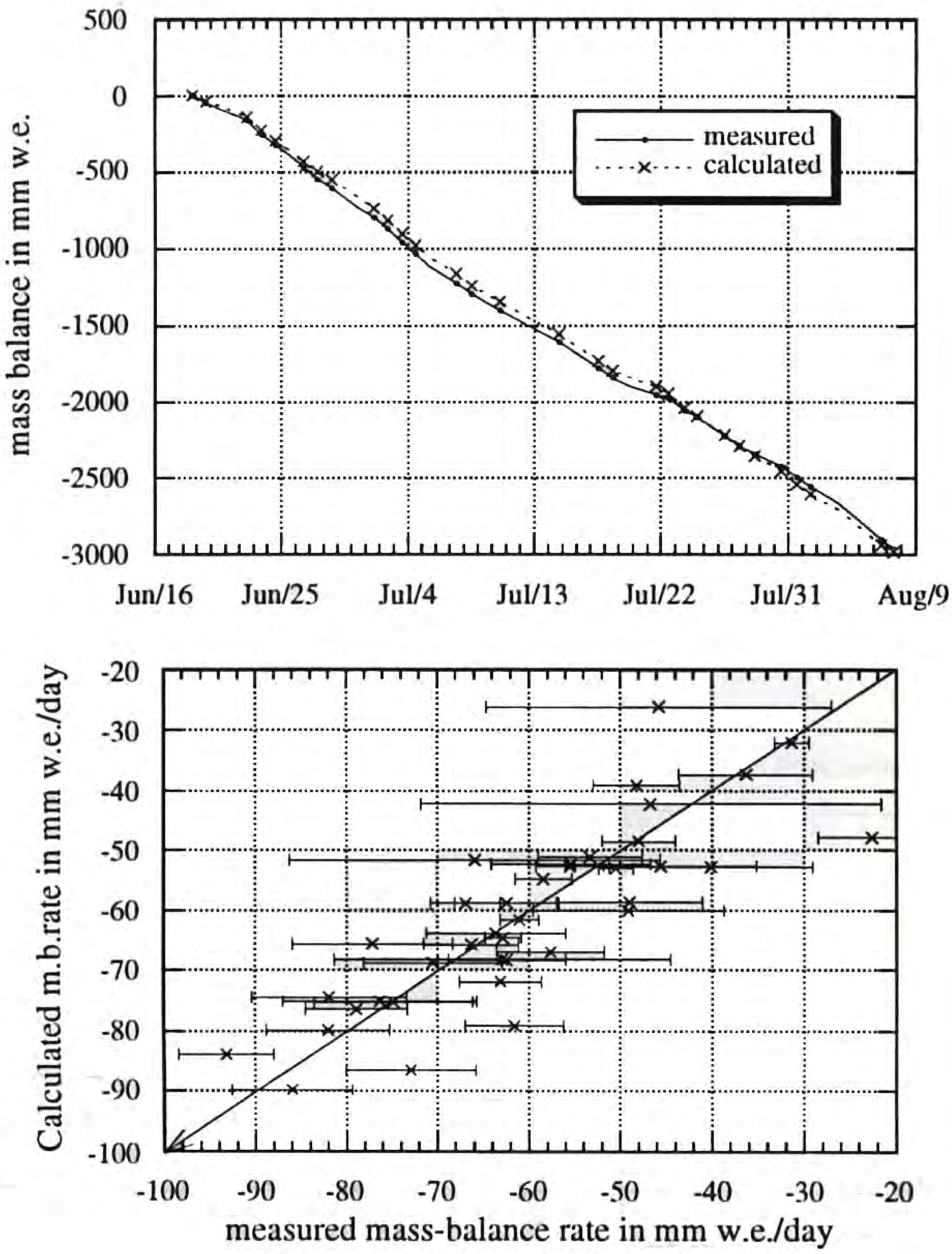


Figure 9: calculated and measured mass balance at A1 (2205 m a.s.l.) between June 18 and August 7, 1994. In the lower panel calculated and measured mass-balance rate during different sub-periods are compared.

Note that the flux averages also shown in Table 5 do not exactly correspond to the values shown in Figure 7 since the periods, over which the averages were computed, differed.

### 2.5.5. Profiles at A1

The profile measurements at A1 show that during PASTEX the dominating winds were katabatic within the first 13 meters above the glacier surface. Profiles of wind speed, temperature and humidity, averaged over the whole period, are shown in Figure 10. The shape of the wind-speed profile is clearly katabatic as it has a distinct maximum between 4 and 8 m. Around this maximum, the temperature profile starts to bend towards a maximum. The humidity profile ends at 8 m. Two times at the beginning of the field experiment, humidity sensors at the top of the mast were damaged owing to lightning, so that the measurement of humidity at 13 m misses for almost the whole period. Nevertheless, the profile looks the same as the temperature profile and will probably show the same bending towards a maximum value.

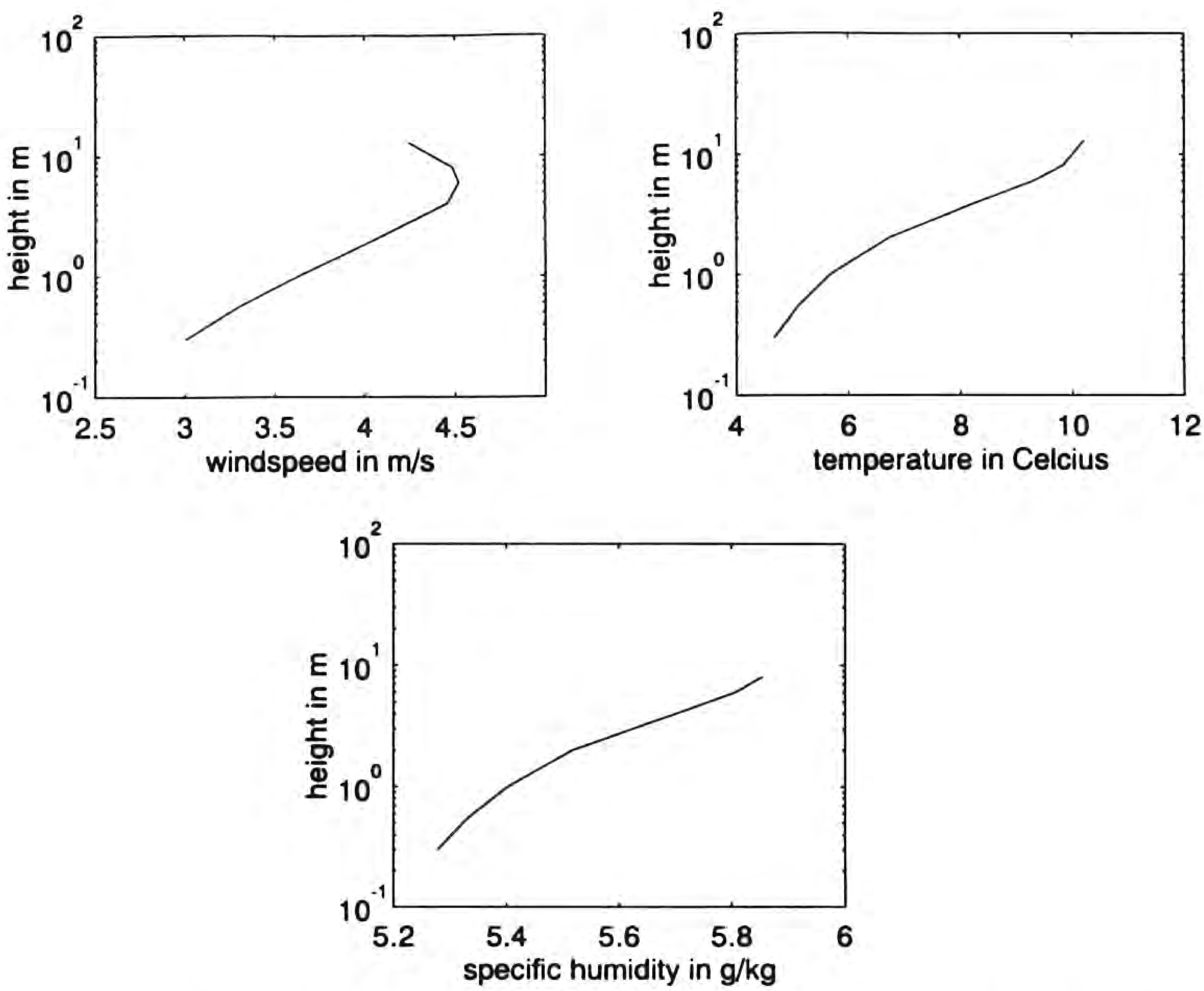


Figure 10: profiles of wind speed, temperature and humidity at A1. These are averages over the whole period of the measurements.

On a day with clear katabatic conditions the wind system shows a diurnal cycle. This is depicted in Figure 11 for August 3. Wind speed and height of the wind-speed maximum increase between 14:00 and 18:00 Local Time and decrease between 21:00 and 24:00 Local Time. This diurnal cycle is due to the diurnal cycle of the air temperature. The resulting temperature difference between the glacier and its surroundings forces the katabatic wind system.

Bintanja, R. et al., 1990: Greenland Ice Margin EXperiment (GIMEX). GIMEX-90 Field report. Internal report of the Institute for Marine and Atmospheric Research, Utr.Un.

Boot, W. et al., 1991: Greenland Ice Margin EXperiment (GIMEX). GIMEX-91 Field report. Internal report of the Institute for Marine and Atmospheric Research, Utr.Un.

Businger, J.A., J.C. Wyngaard, Y. Izumi and E.F. Bradley, 1971: Flux profile relationships in the atmospheric surface layer. *J. Atmos. Sci.*, **28**, 181-189.

Greuell, W. and T. Konzelmann, 1994: Numerical modelling of the energy balance and the englacial temperature of the Greenland Ice Sheet. Calculation for the ETH-Camp location (West Greenland, 1155 m a.s.l.). *Global and Planetary Change*, **9**, 91-114.

Greuell, W. and J. Oerlemans, 1989: Energy balance calculations on and near Hinter–eisferner (Austria) and an estimate of the effect of greenhouse warming on ablation. *Proceedings of the Symposium on Glacier Fluctuations and Climatic Change in Amsterdam. Kluwer Academic Publishers.* ISBN 0-7923-0110-2, p. 305-323.

Koelemeijer, R., J. Oerlemans and S. Tjemkes, 1993: Surface reflectance of Hintereis–ferner, Austria, from Landsat 5 TM imagery. *Annals of glaciology* , **17**, 17-22.

Lang, H. and G.K. Lieb, 1993: Die Gletscher Kärntens. Naturwissenschaftlicher Verein für Kärnten, Klagenfurt.

Munro, D.S. and J.A. Davies, 1977: An experimental study of the glacier boundary layer over melting ice, *J. Glaciol.*, **18**,. 425-436.

Oerlemans, J. and H.F. Vugts, 1993: A meteorological experiment in the melting zone of the Greenland Ice Sheet. *Bulletin of the American Meteorol.Soc.*, **74**(3), 355-365.

Tintor, W., 1991: 10 Jahre Ablationsmesssungen an der Pasterze. *Carinthia II*, **181./101.**, 277-299.

Tintor, W. and H. Wakonigg, 1989: Ein Beitrag zur Kenntnis der vertikalen Bewegungskomponente und des Eisnachschubs an der Pasterze. *Z. Gletscherkd. Glazialgeol.*, **25**(1), 131-137.

Van den Broeke, M.R., P.G. Duynkerke and J. Oerlemans, 1994: The observed katabatic flow at the edge of the Greenland ice sheet during GIMEX-91. *Global and Planetary Change*, **9**, 3-15.

Van de Wal, R.S.W., J. Oerlemans and J.C. Van der Hage, 1992: A study of ablation variations on the tongue of Hintereisferner, Austrian Alps. *J. Glaciol.*, **38**(130), 319-324.

Waba, E., 1993: Eine Parametrisierung der Gletscher-Klima Beziehung. Berechnung der Massenbilanz des Pasterzenkees anhand von Daten der meteorologischen Beobachtungsstation Hoher Sonnblick. Diplomarbeit, Universität Wien.

Wakonigg, H., 1971: Gletscherverhalten und Witterung. *Z. Gletscherkd. Glazialgeol.*, **VII**(1-2), 103-123.

Wakonigg, H., 1991: Die Nachmessungen an der Pasterze von 1879 bis 1990. *Arb. Geogr. Inst. Graz*, **30**, 271-307.

Warrick, R. and J. Oerlemans, 1990: Sea level rise. In: Climate change. The IPCC Scientific Assessment, 257-282. Houghton, J.T. et al. (eds.). Cambridge University Press, Cambridge.

transmission of the instruments must be established. First results of the measurements will be obtained as soon as the calibration has been completed.

Without calibration coefficients it is difficult to judge whether or not the measured signals were realistic. Kipp & Zonen Delft BV, however, established the instrument response (in millivolts; see "sensitivity" in Table 6) to a short-wave radiation flux of 1000 $Wm^{-2}$, so that the LGR output could roughly be compared with the fluxes measured with the Kipp CM 14 on the energy-balance mast at U2. In case of the LDR's , the instrument response was measured from a white field illuminated by a solar flux of 1000 $Wm^{-2}$. Again, this gave a rough idea about the real radiance signal received from the ice surface. Both the LGR's and LDR's proved to give realistic signals.

### 4.4 Period of the measurements

All instruments were flown to U2 on June 15. Comparative measurements and tests were performed from June 18 until 21. The tripods and the LDR's were brought to the slopes S1 and S2 on June 22 and 23. It took some time to solve problems with the software that empties the memory cards. More serious problems were caused by leaking connectors between the instruments and the Campbell data loggers. Water caused short-circuiting and, consequently, loss of data. This proved to be a persistent problem during rainy periods. Treatment of the connectors with spray and tape could prevent substantial data loss. Determination of reliable and unreliable data will be done in the near future. Including some days of unusable data, the measuring period covers June 29 until October 1.

## REFERENCES:

Bachmann, R.C., 1978: Gletscher der Alpen. Hallwag Verlag Bern und Stuttgart.

Bintanja, R., 1995: The local surface energy balance of the Ecology Glacier, King George Island, Antarctica: measurements and modelling. Submitted to Antarctic Science.

Bintanja, R. and M.R. Van den Broeke, 1995: The surface energy balance of Antarctic snow and blue ice. *J. Appl. Meteorol.*, in press.

Bintanja, R., L. Conrads, J. Oerlemans and M. Portanger, 1991: Glacio-meteorological investigations on Ecology Glacier, summer 90-91, King George Island, Antarctica. ARCTOWSKI-90/91 Field Report. Internal report of the Institute for Marine and Atmospheric Research, Utrecht University.

Bintanja, R., M.R. van den Broeke and M.P. Portanger, 1993: A meteorological and glaciological experiment on a blue ice area in the Heimefront Range, Queen Maud Land, Antarctica. SVEA 1992/93 Field report. Internal report of the Institute for Marine and Atmospheric Research, Utrecht University.

### 4.2. Set up

Three stations were established: one on the glacier close to U2, one on the (orographic) left bank near the Hofmannshütte (S1) and one on the right bank close to the Hofmannsweg (S2) (see Figure 2). At U2 upward and downward band irradiances were measured in order to obtain the albedo in Landsat channel 2 (520-600 nm nominal) and channel 4 (760-900 nm nominal). The instruments, pyranometers, were mounted on a mast similar to the "U-masts" described in Section 2.2. The instruments on the two slopes (S1 and S2), pyrheliometers, are identical and measure the radiance received from the ice surface at U2 in the two Landsat channels. These data provide basic input for the calculation of the bi-directional albedo for different view geometry. The instruments were mounted on tripods and erected on grass (S1) and rock (S2). The proper direction of the sensors towards the ice surface of U2 was obtained by looking through a small telescope that was mounted parallel to the pyrheliometers. Table 6 lists relevant characteristics of the instruments. All instruments were sampled by MIDAS (see Section 2.2).

Table 6: overview of the sites and instruments measuring hemispheric and bi-directional albedo in two Landsat channels. LGR and LDR are acronyms for Landsat Global Radiometer and Landsat Direct Radiometer, respectively. The arrows ↓ and ↑ indicate downward and upward directed radiation, respectively. The sensitivity is explained in Section 4.3.

| Station | elevation in m a.s.l. | instrument | variable measured | field of view | sensitivity in mV | Landsat channel |
|---|---|---|---|---|---|---|
| U2 | 2310 | Kipp-LGR1 | irradiance (↓) | 180° | 80 | 2 |
| | | Kipp-LGR2 | irradiance (↑) | 180° | 80 | 2 |
| | | Kipp-LGR3 | irradiance (↓) | 180° | 38 | 4 |
| | | Kipp-LGR4 | irradiance (↑) | 180° | 38 | 4 |
| S1 | 2485 | Kipp-LDR1 | radiance | 5° | 8 | 2 |
| | | Kipp-LDR3 | radiance | 5° | 8 | 4 |
| S2 | 2600 | Kipp-LDR2 | radiance | 5° | 22 | 2 |
| | | Kipp-LDR4 | radiance | 5° | 22 | 4 |

### 4.3. Calibration of the instruments

Unfortunately, time between deliverance of the instruments and beginning of the expedition was too short to allow calibration and testing. Therefore, a "post-expedition" calibration will be performed at the Royal Netherlands Meteorological Institute (KNMI). This calibration consists of measuring the raw output of the instruments against a quartz-halogen lamp with a known spectral irradiance distribution. Besides, the spectral

# 4. MEASUREMENTS OF SPECTRAL ALBEDO

## 4.1. Introduction

Since short-wave radiation is the major source of energy in the energy balance, the albedo is one of the key factors in model calculations. This implies the need for study of the spatial variation of the albedo over the entire surface of the Pasterze. It is obvious that satellite observations offer an excellent opportunity for this. The Landsat Thematic Mapper instrument, with a ground resolution of 30x30 m, provides band radiances from which the surface albedo can be estimated. These radiances must be (1) corrected for interference with the atmosphere, (2) corrected for anisotropic surface reflectance and (3) integrated over the solar spectrum. Such a retrieval method was earlier applied to data of the Hintereisferner (Koelemeijer et al., 1993). It is clear that detailed ground measurements are very important to verify and improve these corrections. Therefore, Kipp & Zonen Delft BV and the IMAU developed a system for measurements of the spectral albedo in Landsat channels 2 and 4, to start with. Together with simultaneously measured values of total (spectral mean) albedo, this allows study of the relation between spectral and spectral mean albedo (relevant for step (3)). Besides, radiances of outgoing radiation were measured, to better understand the anisotropic behaviour of the radiation field that is reflected by the ice surface (step (2)).

The pyrheliometers at S2

A1 for over 90% of the time, and is not restricted to days with fine weather. The glacier wind and especially its influence on the mass balance will be subject of further study.

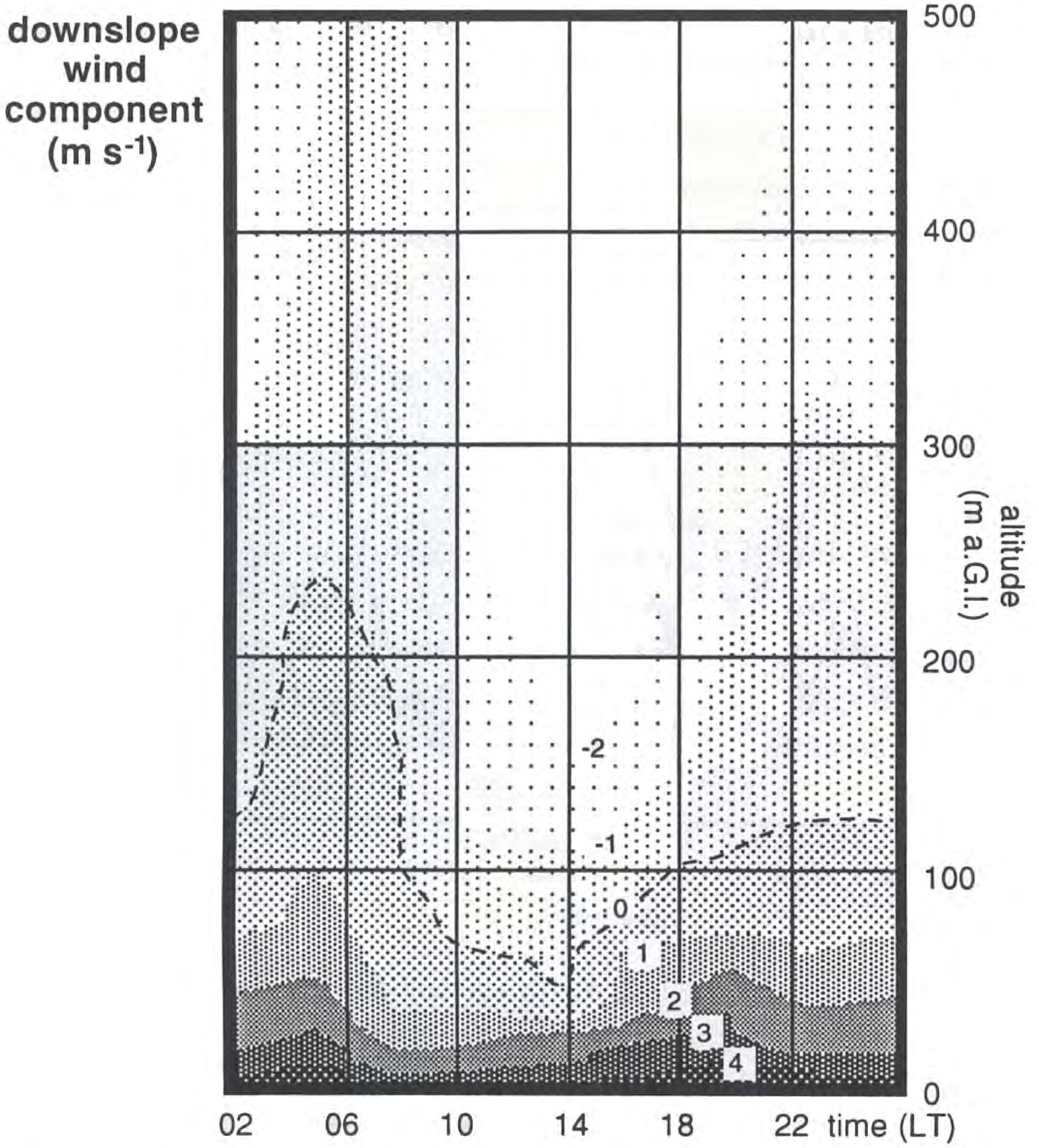


Figure 14: time-height cross section of downslope directed wind component at A1. This is the average for five days with clear weather and weak geostrophic winds.

### 3.4. Preliminary results

Figure 13 shows the noon values of potential temperature at 1, 5, 10, 100 and 500 m above the glacier surface throughout the experiment, based on all available soundings performed at 11h00 and 14h00. Clearly visible is the strong temperature inversion just above the glacier surface, with a very strong increase in potential temperature between 1 and 10 m.

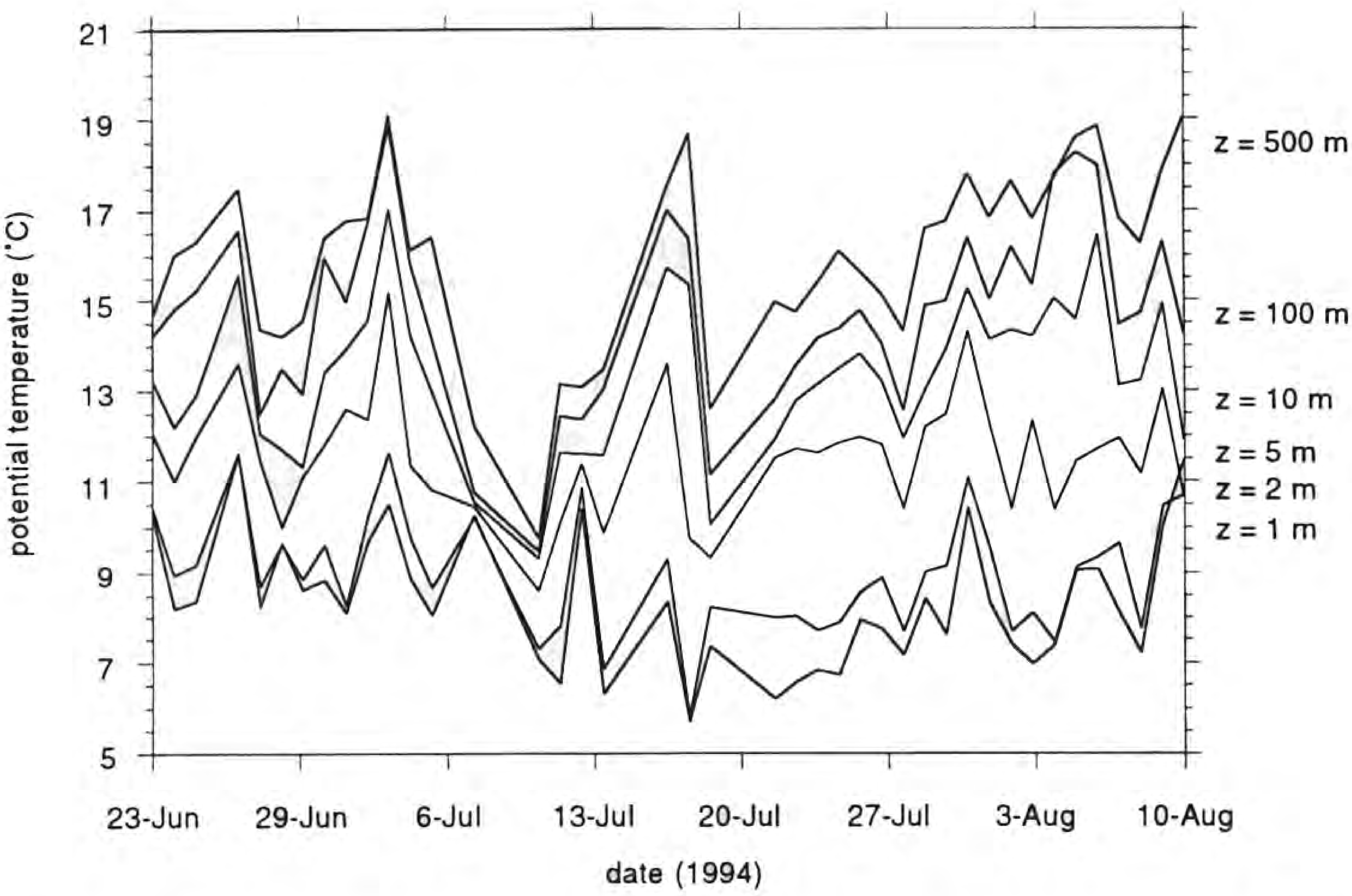


Figure 13: Noon temperatures at 1, 2, 5, 10, 100 and 500 m above the glacier surface.

Because the cold air at the glacier surface is heavier than its surroundings, it starts to flow down the slope. This phenomenon is called "glacier wind" and is a common phenomenon on glaciers. Owing to the size of the tongue of the Pasterze, the glacier wind system is very well developed when compared to other, smaller, valley glaciers. The mean daily cycle of the glacier wind over the 5 days with frequent soundings is presented in Figure 14. The glacier wind has two maxima, one in the early morning and one in the late afternoon. The first one is associated with longwave radiative cooling of the surface, the second with the warm surroundings that increase the temperature contrast between the glacier boundary layer and the free atmosphere. During day time, a clear signature of the valley wind is seen. Like the glacier wind, this is a thermally driven current but it has a larger spatial scale. Preliminary study of the mast data shows that glacier wind is present at

### 3.2. Technical details

When the balloon system is operating, ADAS (Airborne Data Acquisition System) samples the sonde output of atmospheric pressure, temperature, wind speed, wind direction and relative humidity (carbon hygristor) by radio-telemetry every 10 seconds. The receiver operates at 404 MHz. The balloon (Airborne K-65) is filled with 11.3 $m^3$ helium which gives it a lifting power of 17 kg at sea level. The winch has been especially developed for the IMAU and is equipped with a 2500 m Twaron cable (1 g $m^{-1}$, pull strength 250 kg). The large power consumption of the winch (1000 W) made the use of a generator on the ice necessary. During rain or strong winds (>10 m $s^{-1}$), the balloon system cannot be operated: it is a typical "fine weather" system. It was found that in the course of time helium leaks out and air gets into the balloon, reducing the lifting potential. Emptying and refilling the balloon with "fresh" helium solves this problem.

### 3.3. Soundings

Balloon soundings were performed on the glacier at site A1, almost every day at 11:00 and 14:00 Local Time. An overview of the balloon soundings is given in Figure 12. During periods of fine weather, the sounding frequency was increased to once every three hours, while during 5 days the soundings were continued during the night. Depending on the weather conditions and the state of the balloon, the maximum elevation reached was 500-1500 meter above the glacier.

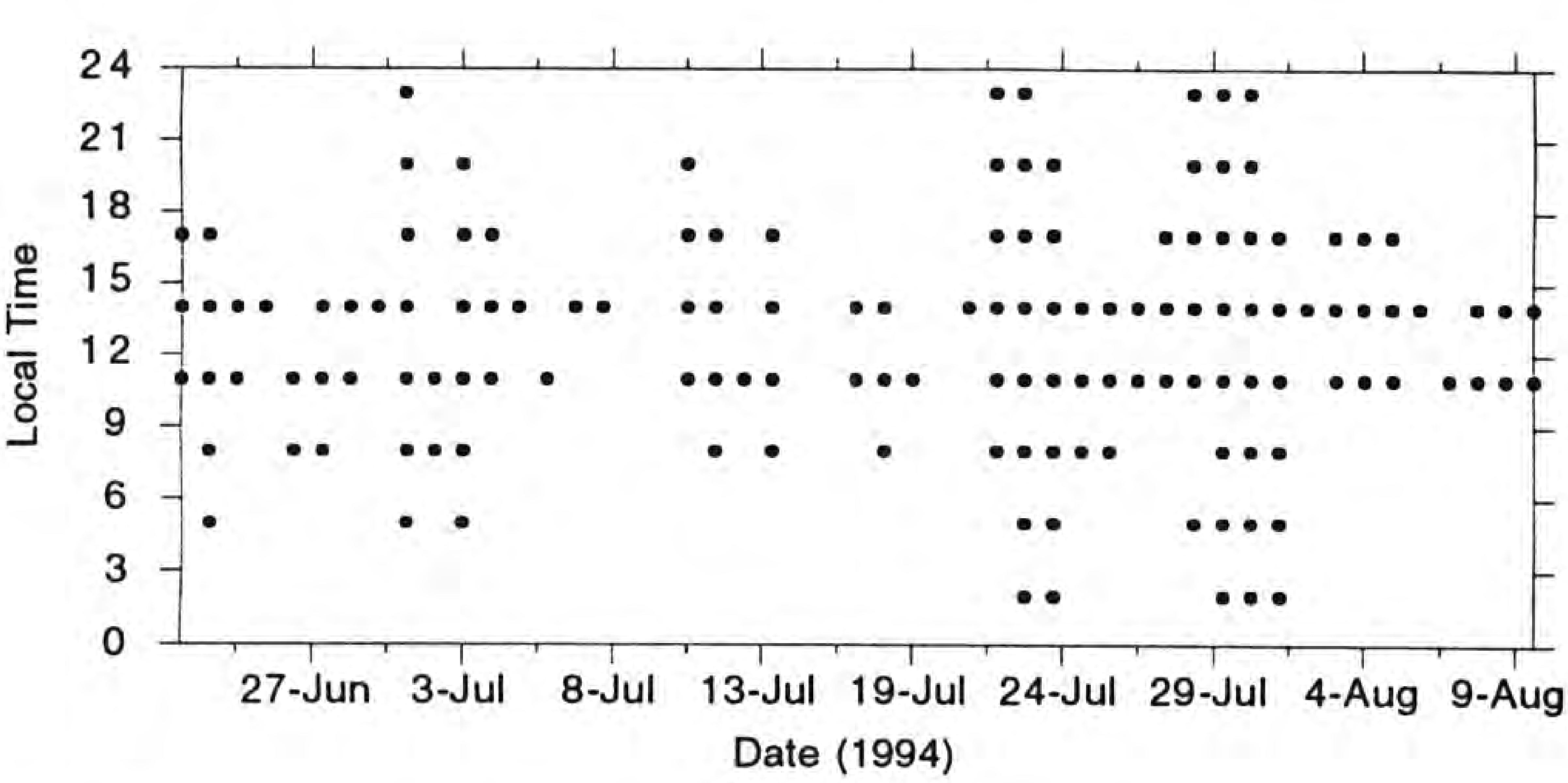


Figure 12: overview of the balloon soundings during the experiment. Every dot represents a sounding.

# 3. BALLOON SOUNDINGS

## 3.1. Introduction

The energy fluxes from the atmosphere towards the glacier surface must go through the atmospheric boundary layer. Vertical sampling of this layer is an important part of any meteorological experiment performed on ice sheets or glaciers. Because the boundary layer is very thin over valley glaciers, typically several to several tens of meters (Munro and Davies, 1977), it was decided to use a tethered balloon instead of standard weather balloons. Standard weather balloons sample the atmosphere up to 20 km or more, but have the disadvantage that they rise very fast. With the present equipment it is possible to regulate the sounding speed from several centimetres to more than one meter per second, so that a detailed insight is gained in the boundary-layer structure. This equipment was used successfully during earlier expeditions to Greenland and Antarctica (e.g. Van den Broeke et al., 1994).

The balloon launching site at A1 (2205 m)

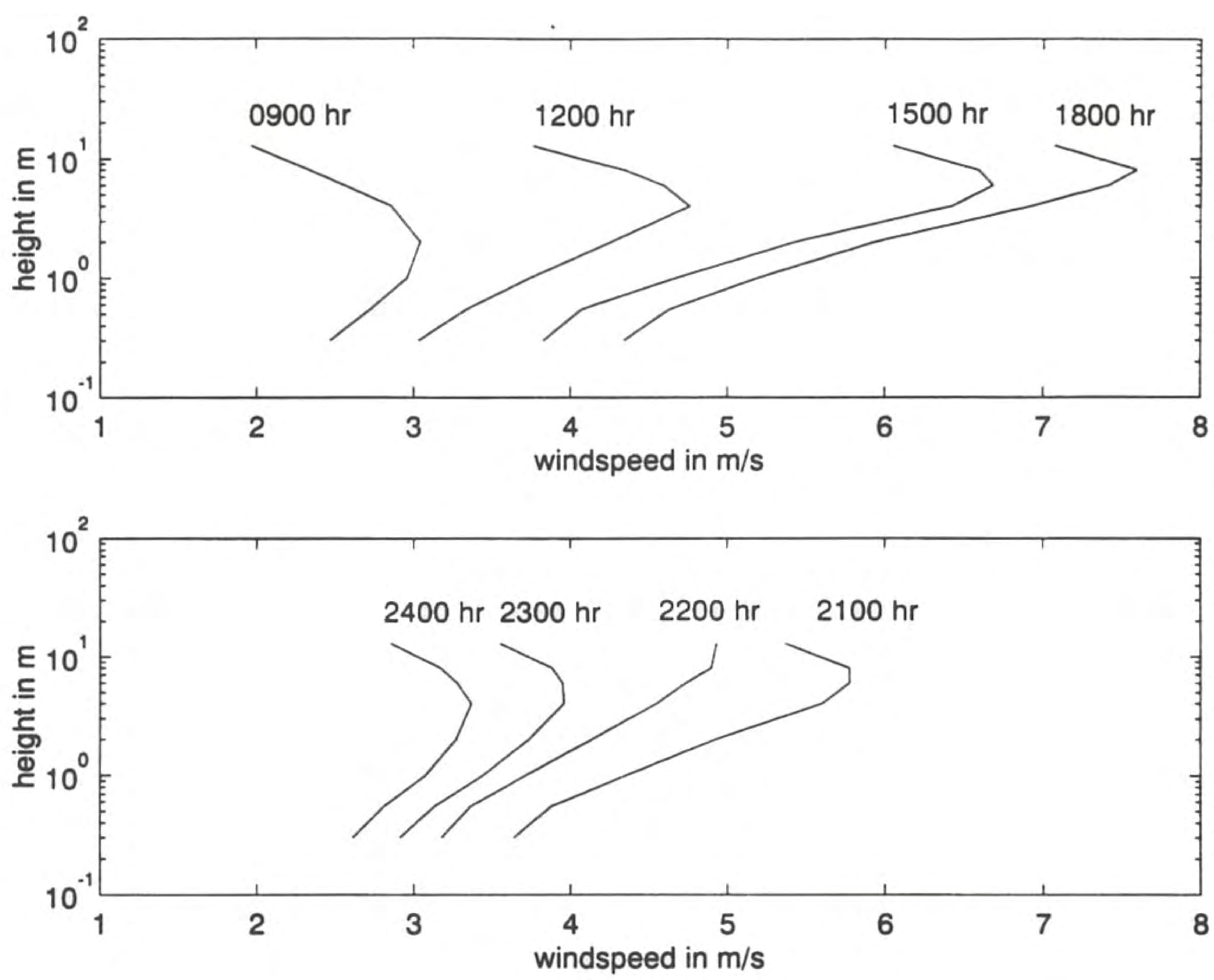


Figure 11: Wind-speed profiles at A1. The curves show half-hourly averages measured on August 3, a day with clear katabatic flow.

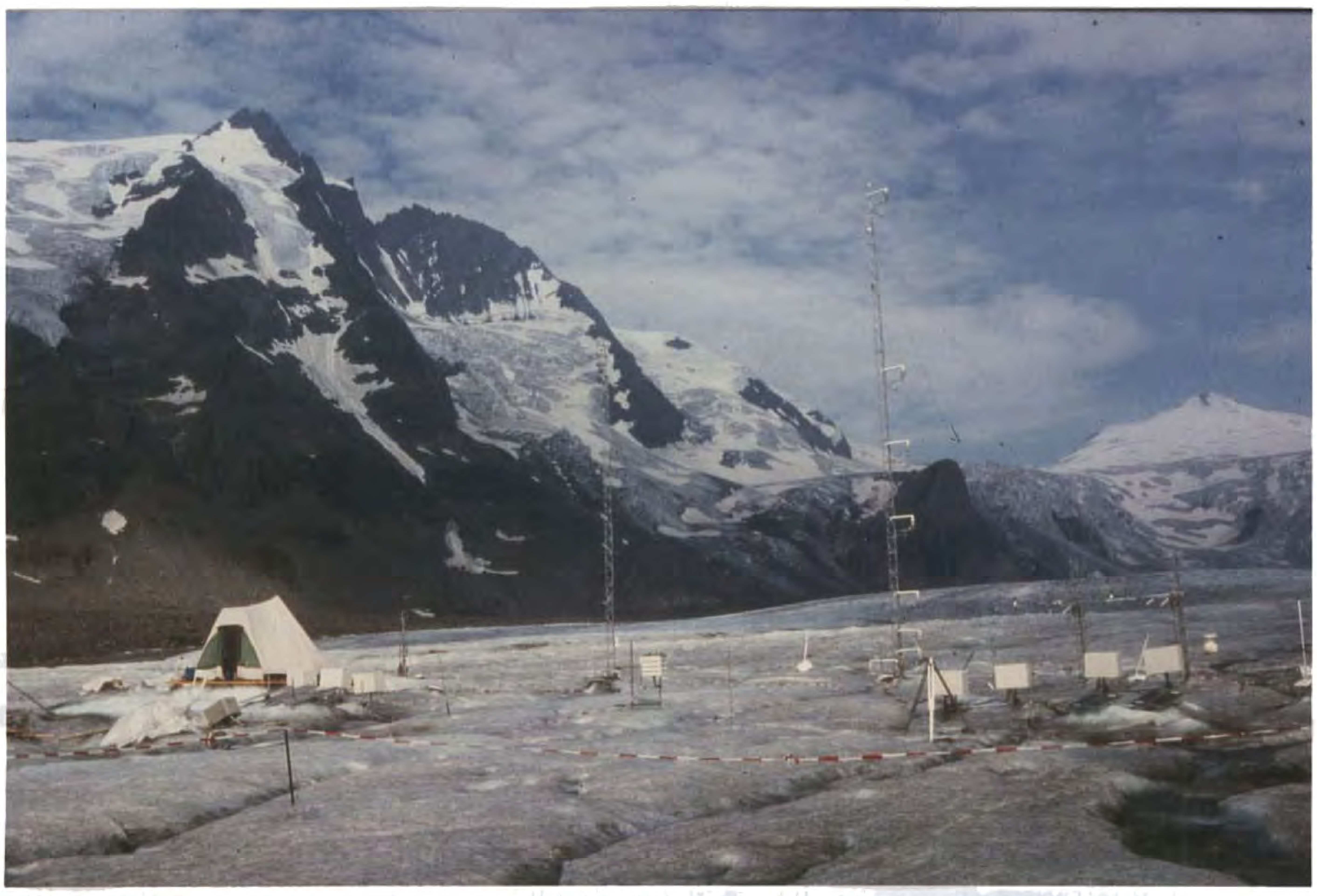

The energy-balance station at A1 (2205 m) with Grossglockner on the background.